Private Fuel Storage, LLC

P.O. Box C4010, La Crosse, WI 54602-4010
John D. Parkyn, Chairman of the Board

July 27, 2000

U.S. Nuclear Regulatory Commission
ATTN: Document Control Desk
Washington, D.C. 20555-0001

LICENSE APPLICATION AMENDMENT No. 15
DOCKET NO. 72-22/TAC NO. L22462
PRIVATE FUEL STORAGE FACILITY
PRIVATE FUEL STORAGE L.L.C.

This letter submits Amendment No. 15 to the Private Fuel Storage Facility (PFSF) License Application (LA). This amendment updates the PFSF Safety Analysis Report (SAR) and Environmental Report (ER) to incorporate several clarifications discussed in a phone call between the NRC, CNWRA and Stone & Webster dated July 21, 2000. The discussion involved: a) the potential for tipping of the storage cask transporter when it is carrying a cask and is postulated to be impacted by the worst case design basis tornado-driven missile; b) the effects of calculated settlement of the Canister Transfer Building on this building's structural integrity; and c) other text clarifications in the SAR and ER.

If you have any questions regarding this submittal, please contact me at 608-787-1236 or Mr. J. L. Donnell, Project Director, at 303-741-7009.

Sincerely,

John D. Parkyn, Chairman
Private Fuel Storage L.L.C.

JDP:JRJ
Enclosure

NMSS01 Public

PREFACE

PRIVATE FUEL STORAGE FACILITY

LICENSE APPLICATION

AMENDMENT 15

Enclosed are the following revisions to the Private Fuel Storage Facility License Application documents:

Safety Analysis Report – Revision 15

Environmental Report – Revision 10

DOCUMENT CONTROL

PAGE	REVISION
Document Control Tab	
a	15
b	15
c	15
d	15
e	15
f	15
g	15
h	15
i	15
j	15
k	15
l	15
m	15
n	15
o	15
p	15
q	15
r	15
s	15
t	15
u	15
v	15
w	15
x	15
y	15
z	15
aa	15
Table of Contents Tab	
i	10
ii	0
iii	9
iv	13
Chapter 1 Tab	
1-i	0
1-ii	0
1.1-1	0
1.1-2	3
1.1-3	3
1.1-4	0
1.2-1	8
1.2-2	8

DOCUMENT CONTROL

PAGE	REVISION
1.3-1	0
1.3-2	0
1.3-3	0
1.3-4	0
1.4-1	4
1.4-2	4
1.5-1	5
1.5-2	0
1.6-1	12
1.6-2	0
1.7-1	12
1.7-2	12
Figure 1.1-1	3
Figure 1.1-2	2
Figure 1.2-1	3
Figure 1.3-1	12
Figure 1.3-2	0
Chapter 2 Tab	
2-i	13
2-ii	13
2-iii	12
2-iv	12
2-v	11
2-vi	11
2-vii	11
2-viii	12
2-ix	13
2-x	11
2-xi	11
2-xii	11
2-xiii	11
2-xiv	11
2.1-1	0
2.1-2	0
2.1-3	6
2.1-4	10
2.1-5	0
2.1-6	0
2.2-1	9
2.2-2	10
2.2-3	9
2.2-4	9
2.2-5	9

DOCUMENT CONTROL

PAGE	REVISION
2.2-6	13
2.2-7	13
2.2-8	13
2.2-9	13
2.2-10	13
2.2-11	13
2.2-12	13
2.2-13	13
2.2-14	13
2.2-15	13
2.2-16	13
2.2-17	13
2.2-18	13
2.2-19	13
2.2-20	13
2.2-21	13
2.2-22	13
2.2-23	13
2.2-24	13
2.3-1	0
2.3-2	0
2.3-3	0
2.3-4	0
2.3-5	0
2.3-6	0
2.3-7	0
2.3-8	0
2.3-9	0
2.3-10	0
2.3-11	0
2.3-12	12
2.3-13	12
2.3-14	12
2.3-15	12
2.3-16	12
2.3-17	12
2.3-18	12
2.3-19	12
2.3-20	12
2.3-21	12
2.3-22	12
2.4-1	0
2.4-2	0
2.4-3	3

DOCUMENT CONTROL

PAGE	REVISION
2.4-4	3
2.4-5	6
2.4-6	3
2.4-7	11
2.4-8	11
2.4-9	11
2.4-10	11
2.4-11	11
2.4-12	11
2.4-13	11
2.4-14	11
2.4-15	11
2.4-16	11
2.5-1	0
2.5-2	3
2.5-3	3
2.5-4	3
2.5-5	15
2.5-6	3
2.6-1	3
2.6-2	3
2.6-3	3
2.6-4	5
2.6-5	3
2.6-6	3
2.6-7	6
2.6-8	6
2.6-9	3
2.6-10	3
2.6-11	3
2.6-12	3
2.6-13	3
2.6-14	3
2.6-15	3
2.6-16	3
2.6-17	6
2.6-18	3
2.6-19	8
2.6-20	15
2.6-21	8
2.6-22	8
2.6-23	8
2.6-24	8
2.6-25	8

DOCUMENT CONTROL

PAGE	REVISION
2.6-26	8
2.6.26a	8
2.6.26b	8
2.6.26c	8
2.6.26d	8
2.6-27	9
2.6-28	9
2.6-29	15
2.6-30	9
2.6-31	11
2.6-32	13
2.6-33	13
2.6-34	13
2.6-35	13
2.6-36	13
2.6-36a	13
2.6-36b	13
2.6-36c	13
2.6-36d	13
2.6-36e	13
2.6-36f	13
2.6-37	13
2.6-38	9
2.6-39	11
2.6-40	11
2.6-41	11
2.6-42	11
2.6-43	11
2.6-44	11
2.6-44a	11
2.6-44b	11
2.6-44c	13
2.6-44d	13
2.6-45	9
2.6-46	13
2.6-47	13
2.6-48	9
2.6-49	13
2.6-50	13
2.6-51	11
2.6-52	9
2.6-53	9
2.6-54	9
2.6-55	13

DOCUMENT CONTROL

PAGE	REVISION
2.6-56	9
2.6-57	13
2.6-58	13
2.6-59	13
2.6-60	9
2.6-61	13
2.6-62	13
2.6-63	13
2.6-64	13
2.6-65	13
2.6-66	13
2.6-67	13
2.6-68	13
2.6-69	9
2.6-70	9
2.6-71	13
2.6-72	15
2.6-72a	15
2.6-72b	15
2.6-73	13
2.6-74	13
2.6-75	13
2.6-76	13
2.6-77	13
2.6-78	13
2.6-79	13
2.6-80	13
2.6-81	13
2.6-81a	13
2.6-81b	13
2.6-82	13
2.6-83	13
2.6-84	9
2.6-85	9
2.6-86	9
2.6-87	11
2.6-88	9
2.6-89	9
2.6-90	9
2.6-91	10
2.6-91a	11
2.6-91b	10
2.6-92	9
2.6-93	9

DOCUMENT CONTROL

PAGE	REVISION
2.6-94	9
2.6-95	9
2.6-96	9
2.6-97	9
2.6-98	13
2.6-99	11
2.6-100	11
2.6-100a	11
2.6-100b	11
2.6-101	9
2.6-102	9
2.6-103	9
2.6-104	9
2.6-105	9
2.6-106	9
2.6-107	9
2.6-108	13
2.6-109	13
2.6-110	9
2.6-111	13
2.6-112	13
2.6-113	11
2.6-114	11
2.6-115	11
2.6-116	9
2.7-1	11
2.7-2	5
2.8-1	11
2.8-2	11
2.8-3	11
2.8-4	11
2.8-5	11
2.8-6	11
2.8-7	12
2.8-8	13
2.8-9	12
2.8-10	15
2.8-11	15
2.8-12	15
2.8-13	15
2.8-14	11
Table 2.3-1	0
Table 2.3-2	0
Table 2.3-3	12

DOCUMENT CONTROL

PAGE	REVISION
Table 2.3-4	12
Table 2.3-5	12
Table 2.3-6	0
Table 2.3-7	0
Table 2.3-8	1
Table 2.3-9	0
Table 2.3-10	0
Table 2.3-11	12
Table 2.6-1	6
Table 2.6-2	6
Table 2.6-3	6
Table 2.6-4 (1 of 14)	0
Table 2.6-4 (2 of 14)	0
Table 2.6-4 (3 of 14)	0
Table 2.6-4 (4 of 14)	0
Table 2.6-4 (5 of 14)	0
Table 2.6-4 (6 of 14)	0
Table 2.6-4 (7 of 14)	0
Table 2.6-4 (8 of 14)	0
Table 2.6-4 (9 of 14)	0
Table 2.6-4 (10 of 14)	0
Table 2.6-4 (11 of 14)	0
Table 2.6-4 (12 of 14)	0
Table 2.6-4 (13 of 14)	0
Table 2.6-4 (14 of 14)	0
Table 2.6-5	6
Table 2.6-6	13
Table 2.6-7	13
Table 2.6-8	13
Table 2.6-9	13
Table 2.6-10	13
Table 2.6-11	13
Table 2.6-12	11
Table 2.6-13	13
Figure 2.1-1	0
Figure 2.1-2 (1 of 2)	3
Figure 2.1-2 (2 of 2)	0
Figure 2.3-1	0
Figure 2.3-2	0
Figure 2.3-3	0
Figure 2.3-4	0
Figure 2.3-5	0
Figure 2.3-6	0
Figure 2.4-1	3

DOCUMENT CONTROL

PAGE	REVISION
Figure 2.4-2	3
Figure 2.4-3	3
Figure 2.4-4	3
Figure 2.4-5	3
Figure 2.5-1	3
Figure 2.6-1	0
Figure 2.6-2 (1 of 2)	8
Figure 2.6-2 (2 of 2)	0
Figure 2.6-3	0
Figure 2.6-4	0
Figure 2.6-5 (1 of 14)	8
Figure 2.6-5 (2 of 14)	8
Figure 2.6-5 (3 of 14)	8
Figure 2.6-5 (4 of 14)	8
Figure 2.6-5 (5 of 14)	8
Figure 2.6-5 (6 of 14)	8
Figure 2.6-5 (7 of 14)	8
Figure 2.6-5 (8 of 14)	8
Figure 2.6-5 (9 of 14)	8
Figure 2.6-5 (10 of 14)	8
Figure 2.6-5 (11 of 14)	8
Figure 2.6-5 (12 of 14)	8
Figure 2.6-5 (13 of 14)	8
Figure 2.6-5 (14 of 14)	8
Figure 2.6-6	0
Figure 2.6-7	0
Figure 2.6-8	0
Figure 2.6-9	0
Figure 2.6-10	0
Figure 2.6-11	0
Figure 2.6-12	0
Figure 2.6-13A	6
Figure 2.6-13B	6
Figure 2.6-13C	6
Figure 2.6-14A	6
Figure 2.6-14B	6
Figure 2.6-14C	6
Figure 2.6-15	0
Figure 2.6-16	0
Figure 2.6-17	6
Figure 2.6-18	6
Figure 2.6-19	8
Figure 2.6-20 (1 of 2)	6
Figure 2.6-20 (2 of 2)	6

DOCUMENT CONTROL

PAGE	REVISION
Figure 2.6-21	6
Figure 2.6-22	6
Figure 2.6-23	6
Figure 2.6-24	6
Figure 2.6-25	11
Figure 2.6-26	6
Figure 2.6-27	6
Figure 2.6-28	6
Figure 2.6-29	6
Figure 2.6-30 (1 of 6)	8
Figure 2.6-30 (2 of 6)	8
Figure 2.6-30 (3 of 6)	8
Figure 2.6-30 (4 of 6)	8
Figure 2.6-30 (5 of 6)	8
Figure 2.6-30 (6 of 6)	8
Figure 2.6-31	11
Appendix 2A Tab	
Reports	8
Appendix 2B Tab	
Survey	0
Appendix 2C Tab	
Analysis	0
Appendix 2D Tab	
Deleted	3
Appendix 2E Tab	
Analysis	0
Appendix 2F Tab	
Report	9
Appendix 2G Tab	

DOCUMENT CONTROL

PAGE	REVISION
Evaluation	10
Chapter 3 Tab	
3-i	9
3-ii	3
3-iii	10
3-iv	10
3-v	0
3-vi	0
3.1-1	0
3.1-2	12
3.1-3	3
3.1-4	1
3.1-5	0
3.1-6	0
3.2-1	0
3.2-2	0
3.2-3	1
3.2-4	1
3.2-5	9
3.2-5a	9
3.2-5b	9
3.2-6	0
3.2-7	9
3.2-8	9
3.2-8a	9
3.2-8b	9
3.2-9	7
3.2-10	5
3.2-11	5
3.2-12	3
3.2-13	12
3.2-14	9
3.2-14a	3
3.2-14b	3
3.2-15	0
3.2-16	3
3.2-17	0
3.2-18	1
3.2-19	1
3.2-20	1
3.2-21	0
3.2-22	0
3.2-23	0

DOCUMENT CONTROL

PAGE	REVISION
3.2-24	0
3.2-24a	12
3.2-24b	12
3.2-25	5
3.2-26	1
3.2-27	1
3.2-28	1
3.2-29	1
3.2-30	1
3.2-31	1
3.2-32	1
3.3-1	0
3.3-2	0
3.3-3	0
3.3-4	0
3.3-5	12
3.3-6	1
3.3-7	13
3.3-8	13
3.3-9	13
3.3-10	10
3.3-11	10
3.3-12	10
3.4-1	0
3.4-2	0
3.4-3	0
3.4-4	9
3.4-5	9
3.4-6	12
3.4-7	12
3.4-8	9
3.5-1	0
3.5-2	0
3.6-1	0
3.6-2	0
3.7-1	12
3.7-2	0
3.7-3	12
3.7-4	12
Table 3.1-1 (deleted)	12
Table 3.1-2 (deleted)	12
Table 3.1-3 (1 of 2, deleted)	12
Table 3.1-3 (2 of 2)	0
Table 3.2-1	12

DOCUMENT CONTROL

PAGE	REVISION
Table 3.2-2	12
Table 3.2-3	0
Table 3.4-1	3
Table 3.6-1 (1 of 5)	12
Table 3.6-1 (2 of 5)	13
Table 3.6-1 (3 of 5)	9
Table 3.6-1 (4 of 5)	12
Table 3.6-1 (5 of 5)	12
Chapter 4 Tab	
4-i	4
4-ii	13
4-iii	10
4-iv	10
4-v	9
4-vi	9
4-vii	9
4-viii	9
4-ix	12
4-x	9
4.1-1	0
4.1-2	0
4.1-3	0
4.1-4	13
4.2-1	0
4.2-2	0
4.2-3	12
4.2-4	12
4.2-5	12
4.2-6	12
4.2-7	12
4.2-8	13
4.2-9	12
4.2-10	12
4.2-11	12
4.2-12	4
4.2-13	1
4.2-14	12
4.2-15	12
4.2-16	12
4.2-16a	7
4.2-16b	12
4.2-16c	10
4.2-16d	7

DOCUMENT CONTROL

PAGE	REVISION
4.2-17	8
4.2-18	12
4.2-19	12
4.2-20	12
4.2-20a	12
4.2-20b	12
4.2-21	4
4.2-22	1
4.2-23	0
4.2-24	0
4.2-25	1
4.2-26	0
4.2-27	0
4.2-28	9
4.2-29	9
4.2-30	7
4.2-31	7
4.2-32	1
4.2-33	7
4.2-34	7
4.2-34a	10
4.2-34b	10
4.2-35	0
4.2-36	0
4.2-37	0
4.2-38	0
4.2-39	9
4.2-40	9
4.2-41	13
4.2-42	9
4.2-43	9
4.2-44	9
4.2-45	9
4.2-46	9
4.2-47	9
4.2-48	9
4.2-49	9
4.2-50	9
4.3-1	9
4.3-2	9
4.3-3	12
4.3-4	13
4.3-5	13
4.3-6	9

DOCUMENT CONTROL

PAGE	REVISION
4.3-7	10
4.3-8	13
4.3-9	13
4.3-10	10
4.3-11	10
4.3-12	13
4.3-13	10
4.3-14	13
4.3-15	13
4.3-16	10
4.3-17	10
4.3-18	10
4.3-19	13
4.3-20	13
4.3-21	13
4.3-22	10
4.4-1	0
4.4-2	0
4.5-1	3
4.5-2	13
4.5-3	2
4.5-4	8
4.5-5	11
4.5-6	11
4.6-1	0
4.6-2	0
4.7-1	0
4.7-2	13
4.7-3	15
4.7-4	0
4.7-5	6
4.7-6	15
4.7-6a	13
4.7-6b	9
4.7-6c	9
4.7-6d	9
4.7-6e	9
4.7-6f	9
4.7-7	9
4.7-8	9
4.7-8a	13
4.7-8b	15
4.7-8c	9
4.7-8d	9

DOCUMENT CONTROL

PAGE	REVISION
4.7-8e	15
4.7-8f	15
4.7-8g	15
4.7-8h	15
4.7-8i	15
4.7-8j	13
4.7-9	3
4.7-10	2
4.7-11	3
4.7-12	9
4.7-12a	9
4.7-12b	9
4.7-13	6
4.7-13a	13
4.7-13b	13
4.7-13c	6
4.7-13d	6
4.7-13e	6
4.7-13f	6
4.7-13g	6
4.7-13h	6
4.7-13i	9
4.7-13j	6
4.7-14	0
4.7-15	12
4.7-16	0
4.7-17	12
4.7-18	0
4.7-19	12
4.7-20	12
4.7-21	12
4.7-22	12
4.7-23	0
4.7-24	1
4.7-25	0
4.7-26	1
4.7-27	6
4.7-28	0
4.7-29	0
4.7-30	0
4.7-31	1
4.7-32	13
4.8-1	12
4.8-2	13

DOCUMENT CONTROL

PAGE	REVISION
4.8-3	0
4.8-4	9
4.8-5	6
4.8-6	15
4.8-7	6
4.8-8	9
4.8-9	13
4.8-10	15
Table 4.1-1 (1 of 7)	1
Table 4.1-1 (2 of 7)	1
Table 4.1-1 (3 of 7)	0
Table 4.1-1 (4 of 7)	0
Table 4.1-1 (5 of 7)	0
Table 4.1-1 (6 of 7)	0
Table 4.1-1 (7 of 7)	0
Table 4.2-1	7
Table 4.2-2	12
Table 4.2-3	12
Table 4.2-4	7
Table 4.2-5	8
Table 4.2-6	9
Table 4.2-7	13
Table 4.2-8	9
Table 4.7-1	12
Table 4.7-2	4
Table 4.7-3	8
Figure 4.1-1	2
Figure 4.1-2	0
Figure 4.1-3	0
Figure 4.1-4	0
Figure 4.2-1	12
Figure 4.2-2 (1 of 3)	12
Figure 4.2-2 (2 of 3)	12
Figure 4.2-2 (3 of 3)	12
Figure 4.2-3	12
Figure 4.2-4	0
Figure 4.2-5 (1 of 4)	0
Figure 4.2-5 (2 of 4)	0
Figure 4.2-5 (3 of 4)	0
Figure 4.2-5 (4 of 4)	0
Figure 4.2-6	0
Figure 4.2-7	8
Figure 4.2-8	0
Figure 4.3-1	11

DOCUMENT CONTROL

PAGE	REVISION
Figure 4.5-1 (1 of 2)	12
Figure 4.5-1 (2 of 2)	12
Figure 4.5-2	0
Figure 4.5-3 (1 of 2)	11
Figure 4.5-3 (2 of 2)	2
Figure 4.5-4	2
Figure 4.5-5	11
Figure 4.5-6 (1 of 4)	3
Figure 4.5-6 (2 of 4)	3
Figure 4.5-6 (3 of 4)	3
Figure 4.5-6 (4 of 4)	3
Figure 4.7-1 (1 of 3)	11
Figure 4.7-1 (2 of 3)	2
Figure 4.7-1 (3 of 3)	11
Figure 4.7-2	0
Figure 4.7-3	0
Figure 4.7-4	0
Figure 4.7-5	3
Figure 4.7-6	3
Figure 4.7-7	6
Figure 4.7-8	11
Chapter 5 Tab	
5-i	0
5-ii	7
5-iii	0
5-iv	0
5-v	0
5-vi	0
5.1-1	0
5.1-2	0
5.1-3	3
5.1-4	2
5.1-5	6
5.1-6	13
5.1-7	13
5.1-8	0
5.1-9	1
5.1-10	13
5.2-1	1
5.2-2	7
5.2-3	7
5.2-4	7
5.2-5	7

DOCUMENT CONTROL

PAGE	REVISION
5.2-6	13
5.3-1	0
5.3-2	0
5.4-1	0
5.4-2	0
5.5-1	1
5.5-2	0
5.6-1	0
5.6-2	0
5.7-1	12
5.7-2	0
Table 5.1-1 (1 of 2)	6
Table 5.1-1 (2 of 2)	6
Table 5.1-2 (1 of 2)	0
Table 5.1-2 (2 of 2)	1
Figure 5.1-1	1
Figure 5.1-2	0
Figure 5.1-3	0
Figure 5.1-4	0
Figure 5.1-5	0
Chapter 6 Tab	
6-i	0
6-ii	0
6.1-1	13
6-1-2	13
6.2-1	1
6.2-2	0
6.3-1	0
6.3-2	0
6.4-1	13
6.4-2	7
6.4-3	7
6.4-4	7
6.5-1	13
6.5-2	0
6.6-1	12
6.6-2	0
Chapter 7 Tab	
7-i	9
7-ii	13
7-iii	10
7-iv	0

DOCUMENT CONTROL

PAGE	REVISION
7-v	0
7-vi	0
7.1-1	0
7.1-2	0
7.1-3	0
7.1-4	0
7.1-5	0
7.1-6	0
7.1-7	0
7.1-8	13
7.1-9	3
7.1-10	3
7.1-11	3
7.1-12	3
7.2-1	10
7.2-2	10
7.2-3	10
7.2-4	10
7.2-5	10
7.2-6	0
7.2-7	10
7.2-8	10
7.2-9	0
7.2-10	10
7.2-11	13
7.2-12	3
7.3-1	0
7.3-2	0
7.3-3	9
7.3-3a	13
7.3-3b	13
7.3-4	10
7.3-5	0
7.3-6	0
7.3-7	10
7.3-8	10
7.3-9	7
7.3-10	12
7.3-11	10
7.3-12	10
7.3-13	10
7.3-14	10
7.3-15	10
7.3-16	10

DOCUMENT CONTROL

PAGE	REVISION
7.3-17	10
7.3-18	10
7.3-19	10
7.3-20	13
7.4-1	7
7.4-2	12
7.4-3	12
7.4-4	12
7.5-1	3
7.5-2	0
7.5-3	8
7.5-4	8
7.5-5	8
7.5-6	8
7.5-7	8
7.5-8	8
7.6-1	12
7.6-2	0
7.6-3	13
7.6-4	13
7.7-1	10
7.7-2	10
7.7-3	10
7.7-4	13
Table 7.3-1	10
Table 7.3-2	10
Table 7.3-3	10
Table 7.3-4	11
Table 7.3-5	10
Table 7.3-6	10
Table 7.3-7	10
Table 7.3-8	10
Table 7.4-1 (1 of 4)	10
Table 7.4-1 (2 of 4)	10
Table 7.4-1 (3 of 4)	10
Table 7.4-1 (4 of 4)	10
Table 7.4-2 (1 of 4)	10
Table 7.4-2 (2 of 4)	10
Table 7.4-2 (3 of 4)	10
Table 7.4-2 (4 of 4)	10
Figure 7.3-1	0
Figure 7.3-2	0

Chapter 8 Tab

DOCUMENT CONTROL

PAGE	REVISION
8-i	0
8-ii	7
8-iii	14
8-iv	9
8-v	9
8-vi	13
8.1-1	9
8.1-2	0
8.1-3	0
8.1-4	0
8.1-5	0
8.1-6	0
8.1-7	7
8.1-8	0
8.1-9	0
8.1-10	12
8.1-11	0
8.1-12	0
8.1-13	0
8.1-14	0
8.1-15	0
8.1-16	13
8.1-17	13
8.1-18	7
8.1-19	7
8.1-20	7
8.2-1	9
8.2-2	3
8.2-3	7
8.2-4	7
8.2-5	12
8.2-6	7
8.2-7	7
8.2-8	7
8.2-9	7
8.2-10	7
8.2-11	7
8.2-12	7
8.2-13	3
8.2-14	3
8.2-15	6
8.2-15a	6
8.2-15b	6
8.2-16	9

DOCUMENT CONTROL

PAGE	REVISION
8.2-17	9
8.2-18	10
8.2-19	10
8.2-20	0
8.2-21	10
8.2-22	13
8.2-23	11
8.2-23a	13
8.2-23b	13
8.2-23c	13
8.2-23d	11
8.2-23e	11
8.2-23f	13
8.2-23g	13
8.2-23h	13
8.2-23i	14
8.2-23j	13
8.2-23k	14
8.2-23l	14
8.2-23m	14
8.2-23n	14
8.2-23o	14
8.2-23p	14
8.2-24	13
8.2-25	13
8.2-26	11
8.2-27	11
8.2-28	13
8.2-29	11
8.2-29a	11
8.2-29b	11
8.2-29c	11
8.2-29d	11
8.2-29e	11
8.2-29f	11
8.2-29g	11
8.2-29h	11
8.2-29i	11
8.2-29j	11
8.2-29k	11
8.2-29l	11
8.2-29m	13
8.2-29n	13
8.2-29o	13

DOCUMENT CONTROL

PAGE	REVISION
8.2-29p	13
8.2-29q	13
8.2-29r	11
8.2-30	5
8.2-31	13
8.2-32	13
8.2-32a	13
8.2-32b	13
8.2-32c	13
8.2-32d	15
8.2-32e	15
8.2-32f	15
8.2-32g	15
8.2-32h	15
8.2-33	15
8.2-34	15
8.2-35	15
8.2-36	3
8.2-37	13
8.2-38	13
8.2-39	3
8.2-40	13
8.2-41	13
8.2-42	13
8.2-43	13
8.2-44	0
8.2-45	12
8.2-46	12
8.2-47	12
8.2-48	7
8.2-49	0
8.2-50	0
8.2-51	9
8.2-52	9
8.3-1	7
8.3-2	7
8.4-1	9
8.4-2	9
8.4-3	9
8.4-4	9
8.4-5	9
8.4-6	9
8.4-7	9
8.4-8	9

DOCUMENT CONTROL

PAGE	REVISION
8.4-9	9
8.4-10	13
8.4-11	13
8.4-12	10
8.5-1	10
8.5-2	9
8.5-3	12
8.5-4	9
8.5-5	9
8.5-6	10
8.5-7	10
8.5-8	13
8.5-9	13
8.5-10	14
Table 8.1-1	9
Table 8.1-2	9
Table 8.2-1	9
Figure 8.2-1	15
Chapter 9 Tab	
9-i	0
9-ii	1
9-iii	4
9-iv	4
9-v	0
9-vi	0
9.1-1	0
9.1-2	0
9.1-3	0
9.1-4	4
9.1-5	4
9.1-6	4
9.1-7	4
9.1-8	4
9.1-9	4
9.1-10	13
9.1-10a	13
9.1-10b	13
9.1-10c	13
9.1-10d	13
9.1-11	13
9.1-12	4
9.1-13	13
9.1-14	0

DOCUMENT CONTROL

PAGE	REVISION
9.1-15	1
9.1-16	1
9.1-16a	1
9.1-16b	1
9.1-17	0
9.1-18	0
9.1-19	0
9.1-20	0
9.1-21	0
9.1-22	0
9.1-23	0
9.1-24	3
9.1-25	4
9.1-26	4
9.1-27	4
9.1-28	4
9.1-29	4
9.1-30	4
9.2-1	13
9.2-2	13
9.2-2a	1
9.2-2b	1
9.2-3	0
9.2-4	0
9.2-5	0
9.2-6	0
9.2-7	1
9.2-8	1
9.2-8a	1
9.2-8b	1
9.3-1	4
9.3-2	4
9.3-3	13
9.3-4	4
9.3-5	4
9.3-6	4
9.3-7	4
9.3-8	4
9.4-1	3
9.4-2	4
9.4-2a	4
9.4-2b	4
9.4-3	3
9.4-4	3

DOCUMENT CONTROL

PAGE	REVISION
9.4-5	3
9.4-6	3
9.4-7	3
9.4-8	3
9.5-1	0
9.5-2	13
9.5-3	0
9.5-4	0
9.6-1	0
9.6-2	0
9.7-1	0
9.7-2	0
9.7-3	0
9.7-4	0
Figure 9.1-1	4
Figure 9.1-2	4
Figure 9.1-3	12
Chapter 10 Tab	
10-i	13
10-ii	13
10.1-1	13
10.1-2	13
Appendix 10A Tab	
Technical Specification Bases	13
Chapter 11 Tab	
11-i	0
11-ii	0
11.1-1	4
11.1-2	4
11.1-3	4
11.1-4	0
11.1-5	0
11.1-6	0
11.1-7	0
11.1-8	0
11.1-9	0
11.1-10	0
11.2-1	0
11.2-2	0

Soil interpretations prepared by USDA (undated) indicate that the permeability of a silt soil in Skull Valley ranges from 0.2 to 0.6 inches/hr. The average groundwater rate of flow was estimated to be approximately 2.8×10^{-3} to 8.5×10^{-3} gallons/day/sq ft. The source of groundwater flow at the site is mainly derived from precipitation that falls at the higher elevations of the Stansbury Mountains. As a result of the low permeability deposits and high evapotranspiration at the site, rainfall at the site is unlikely to contribute to groundwater flow.

Water needs during construction (9,300 gallons/day) and operation (1,800 gallons/day) of the PFSF are modest. During operation, it will be similar to a light industrial facility with a 24-hour a day contingent of security personnel. Highest water demand is associated with the larger daytime work-force as well as operation of a concrete batching plant during initial construction. It is anticipated that surface storage tanks would be erected for potable water, emergency fire water, and for the concrete batching plant, as it is unlikely that water wells drilled into the main valley aquifer would yield adequate quantities of water for these purposes on demand. Several wells on the site may be required to meet the demand. Localized drawdown of the valley aquifer would occur in the vicinity of the wells, the extent of which can not be determined until the wells are drilled, developed, and pump-tested, but which would not extend beyond the site boundary.

Based on initial testing of the onsite monitoring well, it has been determined that operation of the PFSF water well will have no measurable off-site effects on existing groundwater quality or levels (SWEC, 1999b).

2.5.3 Contaminant Transport Analysis

The nature and form of the material stored (spent fuel assemblies in sealed metal canisters) and the method of storage (dry casks) preclude the possibility of a liquid contaminant spill. Discussion of potential contamination of groundwater is not applicable since the depth to groundwater at the site is substantially removed from any activity at the site finished grade.

2.6.1.5 Facility Plot Plan and Geologic Investigations

Figure 2.6-2 is a plot plan showing the locations of the major structures of the PFSF, the locations of the 1996 geotechnical borings and geophysical survey lines, and the location of foundation profiles through the pad emplacement area. Plate 1 of Geomatrix Consultants, Inc. (1999a), indicates the locations of both the 1996 and 1998 investigations, exclusive of the geotechnical borings for the Canister Transfer Building. Figure 2.6-18 shows the locations of the geotechnical borings that were drilled in the vicinity of the Canister Transfer Building in 1998, along with the locations of the CTB foundation profiles.

Geotechnical boring programs were conducted in 1996 and 1998. The borings drilled in October 1996 were located in the pad emplacement area and along the access road corridor, as shown in Figure 2.6-2. The borings drilled in October and December of 1998 were located in the Canister Transfer Building area, as shown in Figure 2.6-18. The soil samples obtained from these borings were sent to the Stone & Webster Geotechnical Laboratory in Boston for testing. The results of the boring programs and laboratory testing are found in Appendix 2A.

In April 1999, ConeTec, Inc performed cone penetration tests (CPT) and dilatometer tests (DMT) in the pad emplacement area and the Canister Transfer Building area. The locations of these CPTs and DMTs are presented in Figure 2.6-19. The results from this subsurface investigation are presented in ConeTec (1999). The primary goal of this investigation was to develop profiles of the relative strength and compressibility of the soils within the depth interval of 10 ft to ~25 ft in the pad emplacement area. As stated in ConeTec (1999), the other interpretations are presented only as a guide for geotechnical use and should be carefully scrutinized for consideration in any geotechnical design.

This program included performing 37 cone penetration tests (CPT) to develop continuous profiles of the strength of the soils in the upper layer (from the surface down to ~25 ft) within the pad emplacement area and 2 under the CTB. Sixteen of these were performed using a seismic CPT to measure down-hole P and S-wave velocities, and the two CPTs performed in the CTB included resistivity measurements. The cone penetration testing program also included performing dilatometer tests (DMT) to develop profiles of the variation of compressibility of the in situ soils. These were located, primarily, in areas where the tip resistance profiles from the CPT tests indicated that the in situ soils had the lowest strengths and the highest compressibilities.

Phase 1 of this program included performing 36 CPTs, located on a grid pattern of ~300 ft within the entire pad emplacement area. This layout provided nine CPTs in each of the four quadrants of the pad emplacement area. Several of these CPTs were located in close proximity to the borings that were drilled previously at the site, permitting correlations between the previous boring and laboratory data to be utilized in the interpretation of the CPT and DMT data. Additional CPTs and DMTs were performed in the vicinity of Borings CTB-4, CTB-5(OW), and C-1, to obtain data for correlating the CPT data with the laboratory testing that was performed on samples from these borings, as well.

The results of the Phase 1 CPTs included measuring continuous profiles of tip resistance and sleeve friction stress, which were used to identify the extent and thickness of the lower blow count soils within the upper layer. The plots of corrected tip resistance, Q_t, vs depth, presented in Appendix E of ConeTec (1999), document the relative strength and compressibility of the soils within the profile. The results are consistent with the results of the borings that were drilled previously at the site; i.e., Q_t increases from grade to a depth of about 15 to 17 ft. Below this depth, it drops slightly

and 6 miles southeast several wells flow at the surface (elevation 4,605 ft). A well at the Tekoi Rocket Engine Test Facility about 3 miles south of the site was drilled to 400 ft and has static water at 80 ft below ground surface (elevation about 4,480 ft). All the above-mentioned wells were completed in unconsolidated materials without drilling into the bedrock. The locations of all wells within 5 miles of the PFSF are identified in Figure 2.5-1. These data suggest that the main aquifer in the central part of Skull Valley is confined or semi-confined and occurs mainly within the fine-grained Tertiary Salt Lake Group deposits. These sediments interfinger with coarse-grained alluvial fan material along the toe of the fan and may create confined conditions where they overlap the fan deposits. The fan deposits are the main recharge zone for the valley aquifers and the main source for domestic water wells in the valley. The aquifer in the fans is unconfined for the most part, but becomes confined and under artesian conditions downslope where the lake and basinal deposits onlap the fan at depth. Water wells drilled near the lower edge of the fan, such as at the Rocket Engine Test Facility, may penetrate several hundred feet of sediments before encountering a coarse alluvial fan layer. Since the coarse layer is under artesian pressure, the level of water in the well will rise upward to the static condition or may flow at the surface, such as occurs just south of the Reservation.

Groundwater levels at the site appear to closely correlate with levels in the main valley aquifer. They do not appear to be affected by proximity to the alluvial fan. At this time it is believed an adequate quantity of suitable quality water can be developed within the site area for the PFSF needs. Specific properties of aquifer materials are unknown at this time. As discussed in ER Sections 4.5.5 - 4.5.7, based on initial testing of the site monitoring well, it is believed that groundwater withdrawals at the PFSF site would have no measurable impact on off-site wells, either up-gradient or down-gradient (SWEC, 1999b). Surface soil at the site has a permeability of 0.2 to 0.6 inch/hr, whereas the soil on the alluvial fan has a permeability of 6 to 20 inches/hr (USDA, unpub. data). As discussed in ER Section 4.5.5, it is estimated that the average withdrawal rate from the well over a 42 year period will be approximately 1,720 gallons per day (1.2 gpm).

Groundwater quality in the area is variable, with the best quality associated with wells developed in the alluvial fans near the Stansbury Mountains. In general, water quality is lower in the valley bottom, but it is suitable for irrigation or stock watering without treatment. The main dissolved ions are sodium and chloride (Hood and Waddell, 1968). There is also a tendency for the quality to be lower farther north, down-valley, towards the Great Salt Lake, although there are exceptions to this trend. Total dissolved solids range from 1,600 to 7,900 mg/l at the northern end of the valley (Arabasz et al., 1987, App. F). Most sources of water in the valley are high in calcium and would be classified as very hard. Aquifer transmissivities range from 500 to 30,000 sq ft/day with an average for Skull Valley estimated at 5,000 sq ft/day (Arabasz et al., 1987, App. F).

2.6.1.10 Geophysical Surveys

Results of seismic refraction and reflection surveys performed at the site in 1996 are found in Appendix 2B. Engineering properties of site materials based on the geophysical investigations are discussed in Section 2.6.1.11. The results of 1998 geophysical surveys (seismic reflection, gravity, and magnetic) are discussed in Geomatrix Consultants, Inc. (1999a) and Bay Geophysical Associates (1999). Seismic cone penetration tests were performed at the locations designated as "SEIS CPT" on Figure 2.6-19. The purpose of these tests was to measure down-hole P and S-wave velocities. The results of these tests are presented in Appendix C of ConeTec, 1999), and the average velocities vs depth are shown in Figure 2.6-28.

Shear wave velocities of soils are dependent on the effective stress, void ratio, and for clays, the plasticity index and overconsolidation ratio of the soils. If all of these parameters were the same, it would be expected that the shear wave velocities would increase with increasing depth in the profile. The apparent leveling off of the shear

LOAD COMBINATION				DISPLACEMENT
Case IIIA	40% N-S,	-100% Vertical,	40% E-W.	0.1 inches
Case IIIB	40% N-S,	-40% Vertical,	100% E-W.	0.4 inches
Case IIIC	100% N-S,	-40% Vertical,	40% E-W.	0.4 inches

The estimated relative displacement of the cask storage pads ranges from ~0.1 inches to 0.4 inches. Because there are no connections between the pads or between the pads and other structures, displacements of this magnitude, were they to occur, would not adversely impact the performance of the cask storage pads. There are several conservative assumptions that were made in determining these values and, therefore, the estimated displacements represent upper-bound values.

The soils in the layer that are assumed to be cohesionless (the one ~10 ft below the pads) are clayey silts and silts, with some sandy silt. To be conservative in this analysis, these soils are assumed to have a friction angle of 30°. However, the results of the cone penetration testing (Appendices D & F of ConeTec, 1999) indicate that these soils have ϕ values that generally exceed 35 to 40°. These high friction angles likely are the manifestation of the cementation that was observed in many of the specimens obtained in split-barrel sampling and in the undisturbed tubes that were obtained for testing in the laboratory. Possible cementation of these soils is also ignored in this analysis, adding to the conservatism.

In addition, this analysis postulates that cohesionless soils exist directly at the base of the pads. In reality, the surface of these soils is 10 ft or more below the pads, and it is not likely to be continuous, as the soils in this layer are intermixed. For the pads to

slide, a surface of sliding must be established between the horizontal surface of the "cohesionless" layer at a depth of at least 10 ft below the pads, through the overlying clayey layer, and daylighting at grade. As shown in the analysis preceding this section, the overlying clayey layer is strong enough to resist sliding due to the earthquake forces. The contribution of the shear strength of the soils along this failure plane rising from the horizontal surface of the "cohesionless" layer at a depth of at least 10 ft to the resistance to sliding is ignored in the simplified model used to estimate the relative displacement, further adding to the conservatism.

These analyses also conservatively ignore the presence of the soil cement under and adjacent to the cask storage pads. As shown above, this soil cement can easily be designed to provide all of the sliding resistance necessary to provide an adequate factor of safety, considering only the passive resistance acting on the sides of the pads, without relying on friction or cohesion along the base of the pads. Adding friction and cohesion along the base of the pads will increase the factor of safety against sliding.

2.6.1.12.2 Stability and Settlement Analyses—Canister Transfer Building

Stability and settlement analyses of the Canister Transfer Building were performed to confirm the adequacy of the structure and its foundation. Calculation 05996.02-G(B)-13 (SWEC, 2000c) evaluated the stability of the Canister Transfer Building and determined it is stable from overturning and/or sliding under the prescribed lateral load conditions. Calculation 05996.02-G(C)-14 (SWEC, 1998) evaluated the soil settlements due to static load conditions and found the resulting building settlements to be uniform and small and to have little effect on the structure. Calculation 05996.02-G(B)-11 (SWEC, 2000d) evaluated the soil settlements due to dynamic load conditions and also found the resulting building settlements to be small and to have little effect on the structure. In summary, the stability and settlement analyses of the

Canister Transfer Building indicates that the building is stable and will retain its structural integrity and the performance of the structure will not be adversely affected.

Chapter 4 describes the structural analyses of the Canister Transfer Building. The analyses used a finite element model approach and considered the effects of soil-structure interaction. The structural analyses take into account the flexibility of the soil underlying the building by the use of finite elements with the stiffness properties of the soil. Non-uniform elastic deformation of the soil, which results in bending moments and shear forces in the base mat are accounted for. This analysis is performed in Calculation 0599602-SC-6 (SWEC, 1998a). Induced stresses resulting from these non-uniform displacements were accommodated in the design of the structure.

The Canister Transfer Building is a large and massive building consisting of exterior reinforced concrete walls 2'-0" thick, a reinforced concrete roof 1'-0" thick, and a solid

THIS PAGE INTENTIONALLY LEFT BLANK

Schmertmann, J. H., 1978, "Guidelines for cone penetration test, performance and design," US Federal Highway Administration, Washington, D.C., Report FHWA TS-78-209, 145.

Scott, W.E., 1988, Temporal relations of lacustrine and glacial events at Little Cottonwood Canyon and Bells Canyon, Utah, in Machette, M.N. and Currey, D.E., editors: In the footsteps of G.K. Gilbert - Lake Bonneville and neotectonics of the eastern Basin and Range Province, guidebook for field trip twelve, Utah Geological and Mineral Survey Misc. Publ. 88-1, pp. 78-82.

Seed, H. B., and Whitman, R. V., 1970, "Design of Earth Retaining Structures for Dynamic Loads," ASCE Specialty Conference on Lateral Stresses in the Ground and the Design of Earth Retaining Structures, pp 103-147.

Silver, M. and Seed, H. B., 1971, "Volume Changes in Sands During Cyclic Loading," Proceedings of the American Society of Civil Engineers, Journal of the Soil Mechanics and Foundations Division, Vol 97, SM9, September.

Simiu, E., M. J. Changery, and J. J. Filliben, 1979, Extreme wind speeds at 129 stations in the contiguous United States, NBS building science series 118: U.S. Department of Commerce, National Bureau of Standards.

Slemmons, D.B., 1980, Design earthquake magnitudes for the western Great Basin, in Proc. of Conference X, Earthquake hazards along the Wasatch-Sierra Nevada frontal fault zones: U.S. Geological Survey Open-file Report 80-801, pp. 62-85.

Smith, R.B., 1978, Seismicity, crustal structure, and intraplate tectonics of the interior of the western Cordillera, in Smith, R.B., and Eaton, G.P., editors, Cenozoic tectonics and regional geophysics of the western Cordillera: Geological Society of America Memoir 152, pp. 111-144.

Smith, R.B., and Arabasz, W.J., 1991, Seismicity of the intermountain seismic belt, in Slemmons, D.B., Engdahl, E.R., Zoback, M.D., and Blackwell, D.C., eds., Neotectonics of North America: Geological Society of America, Decade Map Volume 1, pp. 185-228.

Smith, R.B., and Sbar, M.L., 1970, Seismicity and tectonics of the intermountain seismic belt, western United States, Part II, Focal mechanism of major earthquakes: Geological Society of America Abst. with Programs, vol. 2, p. 657.

Smith, R.B., and Sbar, M.L., 1974, Contemporary tectonics and seismicity of the western United States with emphasis on the intermountain seismic belt: Geological Society of America Bulletin, vol. 85, pp. 1205-1218.

Smith, R.B., Nagy, W.C., Julander, D.R., Viveiros, J.J., Baker, C.A., and Gants, D.G., 1989, Geophysical and tectonic framework of the eastern Basin and Range-Colorado Plateau-Rocky Mountain transition, in Pakiser, L.C., and Mooney, W.D., eds., Geophysical framework of the continental United States: Geological Society of America Memoir 172, pp. 205-233.

Stewart, J.H., 1976, Late Precambrian evolution of North America: plate tectonic implication: Geology, vol. 4, pp. 11-15.

Stewart, J.H., 1978, Basin-range structure in western North America: A review, in Smith, R.B. and Eaton, G.P., editors, Cenozoic tectonics and regional geophysics of the western Cordillera: Geological Society of America Memoir 152, pp. 1-31.

Stickney, M.C., and Bartholomew, M.J., 1987, Seismicity and late Quaternary faulting of the northern Basin and Range province, Montana and Idaho: Seismological Society of America Bulletin, vol. 77, pp. 1602-1625.

Stokes, W.L., 1986, Geology of Utah, Utah Museum of Natural History and Utah Geological and Mineral Survey, Salt Lake City, UT, 280 pp.

Stone & Webster Engineering Corporation (SWEC), 1995. Evaluation of H-Piles, Waste Packaging Area (WPA), and Condensate Demineralizer Waste Evaporator Building (CDWEB), Sequoyah Nuclear Power Plant – Units 1 and 2 (FSAR issues). Tennessee Valley Authority, SE-CEB-SWEC. Calculation No. SCG1S505, Revision 0 (April).

Stone & Webster Engineering Corporation (SWEC), 1998, Calculation No. 05996.02-G(C)-14, Revision 1, Static Settlement of the Canister Transfer Building Supported on a Mat Foundation.

Stone & Webster Engineering Corporation (SWEC), 1998a, Calculation No. 05996.02-SC-6, Revision 0, Finite Element Analysis of Canister Transfer Building.

Stone & Webster Engineering Corporation (SWEC), 1999a, Calculation No. 05996.02-G(B)-12, Revision 1, Flood Analysis with a Larger Drainage Basin.

Stone & Webster Engineering Corporation (SWEC), 1999b, Calculation No. 05996.02-G(B)-15, Revision 1, Determination of Aquifer Permeability from Constant Head Test and Estimation of Radius of Influence for the Proposed Water Well.

Stone & Webster Engineering Corporation (SWEC), 1999c, Calculation No. 05996.02-G(B)-16, Revision 1, Flood Analysis at 3-mile Long Portion of Rail Spur.

Stone & Webster Engineering Corporation (SWEC), 1999d, Calculation No. 05996.02-G(B)-17, Revision 1, PMF Flood Analysis with Proposed Access Road and Rail Road.

Stone & Webster Engineering Corporation (SWEC), 1999e, Calculation No. 05996.02-G(B)-3, Revision 3, Estimate Static Settlement of Storage Pads.

Stone & Webster Engineering Corporation (SWEC), 1999f, Calculation No. 05996.02-SC-5, Revision 1, Seismic Analysis of Canister Transfer Building.

Stone & Webster Engineering Corporation (SWEC), 2000a, Calculation No. 05996.02-G(B)-5, Revision 2, Document Bases for Geotechnical Parameters Provided in Geotechnical Design Criteria.

Stone & Webster Engineering Corporation (SWEC), 2000b, Calculation No. 05996.02-G(B)-4, Revision 6, Stability Analyses of Storage Pad.

Stone & Webster Engineering Corporation (SWEC), 2000c, Calculation No. 05996.02-G(B)-13, Revision 3, Stability Analyses of the Canister Transfer Building Supported on a Mat Foundation.

Stone & Webster Engineering Corporation (SWEC), 2000d, Calculation No. 05996.02-G(B)-11, Revision 1, Dynamic Settlements of the Soils Underlying the Site.

Stover, C.W. and Coffman, J.L., 1993, Seismicity of the United States, 1568-1989 (Revised): U.S. Geological Survey Professional Paper 1527, 418 pp.

Stover, C.W., Reagor, B.G., and Algermissen, S.T., 1986, Seismicity map of the State of Utah, U.S. Geological Survey Miscellaneous Field Studies Map MF-1856, scale 1:1,000,000.

Terzaghi, K, "Evaluation of Coefficients of Subgrade Reaction," Geotechnique, Vol 5, 1955, pp 297-325.

Terzaghi, K., and Peck, R. B., Soil Mechanics in Engineering Practice, John Wiley & Sons, New York, NY, 1967, pp 347 and 491.

Thom, H. C. S., 1963, Tornado probabilities: Monthly Weather Review 91, pp. 730-736.

Tokimatsu, A. M., and H. B. Seed, 1987, "Evaluation of Settlements in Sands Due to Earthquake Shaking," *Journal of the Geotechnical Engineering Division*, ASCE, 113(8), 861-878.

Tooele County Commission, 1995, Brochure entitled "Tooele County, Utah, Where Land And Sky Embrace."

Tooele, 1995. Tooele County General Plan, November 1995.

Tooker, E.W., 1983, Variations in structural style and correlation of thrust plates in the Sevier foreland thrust belt, Great Salt Lake area, Utah, in Miller, D.M., Todd, V.R., and Howard, K.A. editors, Tectonic and stratigraphic studies in the eastern Great Basin: Geological Society of America Memoir 157, pp. 61-73.

Tooker, E.W., and Roberts, R.J., 1971, Structures related to thrust faults in the Stansbury Mountains, Utah: U.S. Geological Survey Professional Paper 750-B, pp. B1-B12.

U.S. Air Force Accident Investigation Board Report, AGM-129 Advanced Cruise Missile, Serial # 90-0061, U.S. Air Force, December 10, 1997, Volume 1.

U.S. Army Corps of Engineers, 1952, Standard Project Flood Determinations, Civil Engineer Bulletin, No. 52-8, Washington, D.C., 19 pp.

U.S. Army Corps of Engineers, 1990, Office of the Chief of Engineers, Flood hydrograph package, HEC-1, Hydrologic Engineering Center, 283 pp.

U.S. Army Corps of Engineers, 1997, Hydrologic Engineering Center, River analysis system, HEC-RAS, Davis, CA.

U.S. Department of Agriculture, undated, Soil survey of Tooele County, Utah, unpublished maps and data, National Resources Conservation Service, Tooele, UT.

U.S. Department of Commerce, National Oceanic and Atmospheric Administration, 1977, Probable maximum precipitation estimates, Colorado River and Great Basin drainage, Hydrometeorological Report No. 49 (HMR 49), 161 pp.

U.S. Geological Survey, 1994, Methods for estimating magnitude and frequency of floods in the southwestern United States, Open-File Report 93-419, 211 pp.

U.S. Nuclear Regulatory Commission, 1991, Safety Evaluation Report related to the operation of Diablo Canyon Nuclear Power Plant Units 1 and 2, NUREG-0675, Supplement No. 34, June 1991.

U.S. Weather Bureau, 1947, Thunderstorm rainfall. Hydrometeorological Report No. 5, Department of Commerce, Washington, D.C., 330 pp.

Vucetic, M., and R. Dobry, 1991, "Effect of Soil Plasticity on Cyclic Response," Journal of the Geotechnical Engineering Division, ASCE, 117(1), 89-107.

Wells, D.L., and Coppersmith, K.J., 1994, Analysis of empirical relationships among magnitude, rupture length, rupture area, and surface displacement: Seismological Society of America Bulletin, vol. 84, pp. 974-1002.

Winterkorn, H. F., and Fang, H., 1975, Foundation Engineering Handbook, Van Nostrand Reinhold Co., New York, NY, 751 pp.

Wong, I., Olig, S., Green, R., Moriwaki, Y., Abrahamson, N., Baures, D., Silva, W., Somerville, P., Davidson, D., Pilz, J., and Dunne, B., 1995, Seismic hazard analysis of the Magna tailings impoundment, in Lund, W.R., ed., Environmental and engineering geology of the Wasatch Front Region: 1995 Symposium and Field Conference, Utah Geological Association Publication 24, pp. 95-110.

Youngs, R.R., Swan, F.H., III, Power, M.S., Schwartz, D.P., and Green, R.K., 1987, Probabilistic analysis of earthquake ground shaking hazard along the Wasatch Front, Utah, in Gori. P.L. and Hays, W.W., editors, Assessment of regional earthquake hazards and risk along the Wasatch Front, Utah: U.S. Geological Survey Open-File Report 87-585, Vol. 2, pp. M-1-110.

Zoback, M.L., 1983, Structure and Cenozoic tectonism along the Wasatch fault zone, in Miller, D.M., Todd, V.R., and Howard, K.A., editors, Tectonic and stratigraphic studies in the eastern Great Basin: Geological Society of America Memoir 157, pp. 3-27.

Zoback, M.L., and Zoback, M.D., 1989, Tectonic stress field of the continental United States, in Pakiser, L.C., and Mooney, W.D., eds., Geophysical framework of the continental United States: Geological Society of America Memoir 172, pp. 523-539.

THIS PAGE INTENTIONALLY LEFT BLANK

4.7.1 Canister Transfer Building

The Canister Transfer Building is provided for physical protection and shielding of the canisters during transfer from the transportation cask to the storage cask. The Canister Transfer Building consists of the shipping cask loading/unloading bays, canister transfer cells, a 200 ton overhead bridge crane, a 150 ton semi-gantry crane, a low level waste storage room, and personnel offices/restroom areas.

The design of the Canister Transfer Building has been performed for critical areas of the structure for the most severe load combinations. Details of the analysis and design are summarized in Section 4.7.1.5.3 Loads provided by the crane vendor have been incorporated in the design and will be verified during the detailed design phase of the project.

No floor drains are located in the Canister Transfer Building to preclude the possibility of contamination entering the septic system. Floor sumps located in the center of each shipping cask load/unload bay, described in Section 4.3.8.1, will collect water from rain and snow that may run off onto the floor from a spent fuel shipment, since the floors are sloped towards the sumps. Collected water will be sampled to ensure no contamination is present prior to removal.

4.7.1.1 Design Specifications

The building will be designed in accordance with the Principal Design Criteria contained in Chapter 3. The Canister Transfer Building is a massive reinforced concrete structure with thick walls provided for tornado-generated missile protection and radiation shielding. The building will be designed in accordance with the provisions of ACI-349 (Reference 15).

4.7.1.2 Plans and Sections

The Canister Transfer Building is shown in Figure 4.7-1.

4.7.1.3 Function

The function of the Canister Transfer Building is to assist in the canister transfer operations at the PFSF. A description of the canister transfer operations is contained in Chapter 5.

Canister Transfer Building functions include:

- Load or unload spent fuel shipping casks from the heavy haul tractor/trailers.
- Provide weather and tornado proof protection for performing the canister transfer operations.
- Provide the support structure for the single failure-proof cranes required for the transfer operations.
- Provide radiological shielding during the transfer operation.
- Store potential low-level radioactive waste from health physics surveys.
- Provide storage and laydown space for transfer and shipping equipment.
- Provide a staging area for storage casks.

4.7.1.4 Components

The major components that comprise the Canister Transfer Building are the cask loading/unloading bays, three canister transfer cells, the 200 ton overhead bridge crane, the 150 ton semi-gantry crane, crane runway girders and their supports, cask transporter bay, tornado-missile barriers, low level waste storage room, radiation shield

walls and doors, equipment lay-down areas, storage cask delivery and staging platform, mechanical and electrical equipment areas, and personnel offices and restroom areas.

4.7.1.4.1 Seismic Support Struts

The seismic support struts are rigid strut assemblies that secure the shipping and transfer casks to the Canister Transfer Building columns during transfer operations. The struts ensure that the casks will remain stable and will not topple in the event of an earthquake. The struts are designed to resist the horizontal forces due to the seismic accelerations developed in the seismic analysis of the building (Reference 62). The casks do not require seismic restraint in the vertical direction since the upward seismic forces are less than the deadweight of the casks.

The struts are connected to the shipping cask after it is moved into the transfer cell. Struts are also attached to the transfer cask when it is placed on top of the shipping cask or storage cask, prior to disconnecting the transfer cask from the crane. Each cask utilizes two struts, vertically positioned near the cask center of gravity, that provide lateral restraint in two orthogonal directions. Figure 4.7-7 is a schematic diagram of the support struts.

The support struts are procured as standard sway strut assemblies that conform to ASME III, NF requirements for Class 2 nuclear grade supports. The struts consist of a rigid tubular body with threaded eye rods on both ends. Each strut is pinned to a bracket that is secured to the cask and to the building columns. At the building columns, the brackets are welded to steel plate secured to the column with anchor rods.

4.7.1.5 Design Bases and Safety Assurance

The Canister Transfer Building is classified as being Important to Safety to provide the safety assurance commensurate with canister transfer activities. The design bases for the Canister Transfer Building are described in Chapter 3.

4.7.1.5.1 Structural Design

The building structure has been analyzed and critical areas have been designed for the critical loads cases. A design evaluation determined the worst loading case and areas of the structure. The rationale for selection of the worst loading case for the evaluation is provided below:

The load combinations for reinforced concrete design of the Canister Transfer Building, given in Section 3.2.11.4.1 are as follows:

a.) $U_c > 1.4\ D + 1.7\ L$

b.) $U_c > 1.4\ D + 1.7\ L + 1.7\ H$

c.) $U_c > 0.75(1.4\ D + 1.7\ L + 1.7\ H + 1.7\ T)$

d.) $U_c > 0.75\ (1.4\ D + 1.7\ L + 1.7\ H + 1.7\ T + 1.7\ W)$

e.) $U_c > D + L + H + T + E$

f.) $U_c > D + L + H + T + A$

g.) $U_c > D + L + H + T + W_t$

h.) $U_c > D + L + H + T + F$

H. Lightning

The Canister Transfer Building is approximately 77 feet tall and is a possible lightning target. A lightning Risk Assessment performed in accordance with NFPA 780 determined that the Canister Transfer Building at the PFSF has a "moderate to severe risk factor." The risk assessment was based on the following criteria:

- The building houses the handling of hazardous materials
- The building construction consists of reinforced concrete w/ concrete roof
- The building extends more than 50 ft above adjacent structures or terrain
- The area topography is flat ground
- The building contains critical operating equipment
- The lightning frequency Isoceraunic level for the site location in Utah has 31 – 40 mean annual number of days with thunderstorms

Therefore the Canister Transfer Building will be designed with lightning protection features in accordance with NFPA 780. An air terminal lightning protection system will be installed on the building to protect the building from damage from a lightning strike. Air terminals will be erected on the ridge and perimeter of the upper roof and on the perimeter and interior of the lower roof areas. The air terminals will be interconnected to a main conductor cable that will provide a two-way path to ground for any of the terminals. The main conductor cable will be connected to down conductors that extend to ground rods around the perimeter of the building. All lightning protection materials will use NFPA 780 Class II materials since the building exceeds 75 ft in height. A lightning protection system as described above will ensure that lightning strikes will not prevent any SSCs that are important to safety from performing their safety function.

4.7.1.5.2 Shielding Design

The Canister Transfer Building is designed to provide radiological shielding during the transfer operations. A portion of the building is divided into canister transfer cells where the transfer operations are performed. The cells are surrounded by concrete shield walls that are designed to limit the radiation doses from the canister transfer operations to personnel outside of the cell to 2 mrem/hr, which is below the 5 mrem/hr dose level

that establishes a "radiation area" per 10 CFR 20.1003. Large sliding doors for moving shipping and storage casks in and out of the cell are made of steel with a polyethylene (or similar) shield, as necessary, to minimize neutron doses. Personnel access openings into the cells are designed with a labyrinth of concrete to mitigate streaming of radiation. The walls and sliding doors of the canister transfer cells shall be seismically designed to withstand earthquake induced loads and remain in place following the PFSF design basis ground motion.

A shielding analysis will be performed assuming canisters containing design basis fuel involved in canister transfer operations to determine transfer cell wall and cell door thickness requirements. The analysis will consider attenuation of the radiation doses through the shield walls and doors to locations outside the cell.

4.7.1.5.3. Structural Analysis

The design of the Canister Transfer Building included the conceptual drawings shown in the Figure 4.7-1 and design criteria identified in Chapter 3 and summarized in Table 3.6-1. The methodology and reference standards identified for use in the building seismic analysis is described in Section 3.2.10. Load combinations for the building design are shown in Section 3.2.11.4.

The first consideration in the design was the selection of the critical load combinations. It was judged that the critical load cases would be those including the ISFSI design basis ground motion, since the building is subjected to high seismic loads and relatively low (Zone 3) tornado loads. A seismic analysis of the structure was performed to determine the seismic loads for the building design, and to generate in-structure response spectra for the design of the overhead bridge crane and semi-gantry crane, both supported on the Canister Transfer Building walls. The seismic analysis was performed following the guidelines of ASCE-4 (Reference 20). To perform the analysis,

Two critical load cases were considered. The first is that which produces the worst downward loading on the roof, and includes dead load, live load, and the vertical seismic load acting downward. The vertical seismic load is developed by applying as a static load the enveloped ZPA accelerations from the seismic analysis to the mass of the structure. Included in this load combination is 40% of the enveloped ZPA acceleration in each of the two horizontal (N-S and E-W) directions. This load combination governs the design of the roof, some of the walls, and portions of the base mat. The second load case was selected because it had the greatest overturning potential. It includes dead load, reduced live load, the enveloped E-W ZPA acceleration, 40% of the enveloped vertical ZPA acceleration upward, and 40% of the enveloped ZPA acceleration in the N-S direction. This load combination governs the design of portions of the base mat, crane support beams and some walls. Selected results of the analyses are presented in Figures 10 through 16. The finite element analysis, including the soil model and building model, is described in calculation SC-6 (Reference 46).

Results of the analysis were used to design the reinforcing steel for the concrete walls, slabs, beams and columns (pilasters). In general, the reinforcing required was not excessive. Highly stressed areas are in the roof slab, in the N-S walls where the roof beams intersect the wall, in the crane support beams, in the E-W shear walls, and in the corners of the base mat. The design of the reinforcing steel is described in calculation SC-7 (Reference 47).

<u>Mat Foundation Stability Analyses and Settlement</u>

In addition to the structural analyses described above, stability and settlement analyses of the Canister Transfer Building were also performed to confirm the adequacy of the structure and its foundation. Calculation 05996.02-G(B)-13 (Reference 48) evaluated the stability of the Canister Transfer Building and determined it is stable from overturning and/or sliding under the prescribed lateral load conditions. Calculation

05996.02-G(C)-14 (Reference 49) evaluated the soil settlements due to static load conditions and found the resulting building settlements to be uniform and small and to have little effect on the structure. Calculation 05996.02-G(B)-11 (Reference 84) evaluated the soil settlements due to dynamic load conditions and also found the resulting building settlements to be small and to have little effect on the structure. In summary, the stability and settlement analyses of the Canister Transfer Building indicates that the building is stable and will retain its structural integrity and the performance of the structure will not be adversely affected.

As part of the stability analyses, soil bearing capacity evaluations were performed for the mat founded on soils that were conservatively assigned average undrained shear strengths and effective-stress strength parameters applicable for the soils in the upper ~25 to ~30 ft layer at the site. The strengths of the underlying soil layers are much greater than are applicable for the upper layer; therefore, assuming that they have the same strengths provides a conservative, lower-bound assessment of their stability. See Section 2.6.1.11 for a detailed discussion of the static and dynamic strengths of the soils underlying the site and Section 2.6.1.12.2 for a detailed discussion of the stability analyses of the Canister Transfer Building.

Several load cases were considered in the stability analyses, which consisted of combinations of vertical static, vertical seismic in upward and downward directions, and horizontal seismic in E-W and N-S directions. Loads developed in Calculation SC-5 (Reference 44) were used in these analyses. As in the structural analyses discussed earlier, seismic loads used were based on 100% of the enveloped ZPA acceleration in one direction, combined with 40% of the enveloped ZPA accelerations in each of the other two directions. Minimum factors of safety of 3.0 for the static load case and 1.1 for the seismic load cases are required against a bearing capacity failure of the foundation in soil.

Tables 2.6-9 and 2.6-10 present the results of the bearing capacity analyses of the

Canister Transfer Building. Table 2.6-9 indicates that the factor of safety for the static load case is greater than 11, which exceeds the minimum required factor of safety of 3.0 by a wide margin. Table 2.6-10 presents the results of the dynamic bearing capacity analyses. It indicates that Load Case IIIB, the load combination of full static, 40% horizontal seismic in N-W direction, 40% seismic uplift, and 100% horizontal seismic in E-W, is the most critical load case. This load case results in an actual soil bearing pressure of 3.3 kips per square foot (ksf), compared with an ultimate bearing capacity of 9.9 ksf. The resulting factor of safety against a bearing capacity failure for this load case is 3, compared with the minimum allowable factor of safety for seismic loading cases of 1.1. Therefore, there is an adequate factor of safety against a bearing capacity failure due to static and dynamic loads.

The sliding stability of the Canister Transfer Building is discussed in detail in Section 2.6.1.12.2. The Canister Transfer Building will be founded on clayey soils that have an adequate amount of cohesion to resist sliding due to the dynamic forces from the design basis ground motion. A 1-ft deep key will be constructed around the perimeter of the mat to ensure that the full shear strength of the clayey soils is engaged to resist sliding of the structure due to loads from the design basis ground motion. As shown in Figures 2.6-21 through 2.6-23, however, some of the soils underlying the building may be cohesionless within the depth zone of about 10 to 20 ft, especially near the southern portion of the building. Analyses were performed to address the possibility that sliding may occur along a deeper slip plane at the clayey soil/sandy soil interface as a result of the earthquake forces. These analyses indicate that the factor of safety against sliding along the top of this layer is >1.1 for Load Cases IIIA and IIIC and they illustrate that it is ~1.1 for Load Case IIIB.

These analyses include several conservative assumptions. They are based on static strengths of the silty clay block under the Canister Transfer Building mat, even though experimental results indicate that the strength of cohesive soils increases as the rate of

loading increases. For rates of strain applicable for the cyclic loading due to the design basis ground motion, for most practical cases, one can assume that $c_{u\,dynamic} \sim 1.5 \times c_{u\,static}$. In addition, the silty sand/sandy silt layer is not continuous under the Canister Transfer Building mat, and this analysis neglects cementation of these soils that was observed in the samples obtained in the borings. Therefore, sliding is not expected to occur along the surface of the cohesionless soils underlying the Canister Transfer Building.

An additional analysis of sliding was performed to define the upper bound of potential movement that might occur due to the earthquake. In this analysis it was postulated that the cohesionless soils extend above the depth of about 10 ft and the structure is founded directly on the cohesionless materials. This analysis conservatively assumed that $\phi = 35°$ and $c = 0$ for these soils. Because of the magnitude of the dynamic forces resulting from the soil-structure interaction analyses, the factor of safety against sliding of this building would be less than 1 if it were founded on cohesionless soils. Where the factor of safety against sliding is less than 1, the displacements the building may experience were calculated using the method proposed by Newmark (1965) for estimating displacements of dams and embankments during earthquakes.

In these analyses, several conservative assumptions were made, and even with this high level of conservatism, the estimated relative displacement of the building ranged from 0.5 inches to 1.2 inches. Motions of this magnitude, occurring at the depth of the silty sand/sandy silt layer, would likely not even be evident at the ground surface. For the building to slide, a surface of sliding must be established between the horizontal sliding surface in the silty sand/sandy silt layer and through the overlying silty clay/clayey silt layer. In the simplified model used to estimate these displacements, the contribution of this surface of sliding through the overlying silty clay/clayey silt layer to the dynamic resistance to sliding motion is ignored, as is the passive resistance that would act on the embedded portion of the building foundation and the block of soil that

is postulated to be moving with it. It is likely, moreover, that should such slippage occur within the cohesionless soils underlying the building, it would minimize the level of the accelerations that would be transmitted through the soil and into the structure. In this manner, these cohesionless soils would act as a built-in base shear isolation system. Any decrease in these accelerations as a result of this would decrease the inertial forces of the building, which would diminish the estimated displacements as well. Further, since there are no important-to-safety systems that would be severed or otherwise impacted by movements of this small amount as a result of the earthquake, such postulated, minute movements do not adversely affect the performance of the Canister Transfer Building.

THIS PAGE INTENTIONALLY LEFT BLANK

35. NUREG-0612, Control of Heavy Loads at Nuclear Power Plants, U.S. Nuclear Regulatory Commission, July 1980.

36. Silva, W.J., and Lee, K., 1987, WES RASCAL code for synthesizing earthquake ground motions: State-of-the-art for assessing earthquake hazards in the United States: U.S. Army Waterways Experiment Station, Report 24, Miscellaneous Paper S-73-1, 120 p.

37. Lilhanand, K., and Tseng, W.S, 1988, Development and Application of Realistic Earthquake Time Histories Compatible with Multiple-Damping Response Spectra: Ninth World Conference on Earthquake Engineering, Tokyo, Japan, v. II, 819-824.

38. NUREG-0800, Standard Review Plan for the Review of Safety Analysis Reports for Nuclear Power Plants, U.S. Nuclear Regulatory Commission, Revision 2, 1989.

39. PFSF Calculation No. 05996.02-G(PO18)-3, Geomatrix Consultants, Inc., Development of Time Histories for 2,000-Year Return Period Design Spectra, (Rev 0), August 1999.

40. PFSF Calculation No. 05996.02-G(PO18)-2, Soil and Foundation Parameters for Dynamic Soil-Structure Interaction Analyses, 2,000-Year Return Period Design Ground Motion, Revision 0, Stone & Webster.

41. REFUND, Stone & Webster computer program, ST-232, Ver-0, Level 1.

42. PFSF Calculation No. 05996.02 SC-4, Development of Soil Impedance Functions for Canister Transfer Building, Revision 1, Stone & Webster.

43. FRIDAY, Stone & Webster computer program, ST-243, Ver-02, Level 01.

44. PFSF Calculation No. 05996.02 SC-5, Seismic Analysis of Canister Transfer Building, Revision 1, Stone & Webster.

45. ANSYS computer program, Version 5.4, Swanson Analysis Systems, Inc.

46. PFSF Calculation No. 05996.02 SC-6, Finite Element Analysis of Canister Transfer Building, Revision 0, Stone & Webster.

47. PFSF Calculation No. 05996.02 SC-7, Design of Reinforcing Steel for Canister Transfer Building, Revision 0, Stone & Webster.

48. PFSF Calculation No. 05996.02 G(B)-13, Stability Analyses of the Canister Transfer Building Supported on a Mat Foundation, Revision 3, Stone & Webster.

49. PFSF Calculation No. 05996.02 G(C)-14, Static Settlement of the Canister Transfer Building Supported on a Mat Foundation, Revision 1, Stone & Webster.

50. (deleted)

51. Generic Licensing Topical Report for Ederer's Nuclear Safety Related eXtra Safety And Monitoring (X-SAM) Cranes, EDR-1(NP)-A, Ederer Incorporated, Revision 3, October 1982.

52. Appendix B Supplement to Generic Licensing Topical Report EDR-1, Summary of Facility Specific Crane Data Supplied by Ederer Incorporated for PFSF, 200/25 Ton Bridge Crane, Revision 0, November 1998.

71. Stone & Webster Engineering Corporation (SWEC), 2000a, Calculation No. 05996.02-G(B)-5, Revision 2, Document Bases for Geotechnical Parameters Provided in Geotechnical Design Criteria.

72. NFPA-801, Standard for Fire Protection for facilities Hanlding Radioactive Materials, 1998.

73. NFPA-220, Standard on Types of Building Construction, 1995.

74. NUREG-0908, Acceptance Criteria for the Evaluation of Nuclear Power Reactor Security Plans, 1982.

75. NUREG/CR-0509, Emergency Power Supplies for Physical Security Systems, November 1979.

76. NFPA-37, Standard Installation and Use of Stationary Combustion Engines and Gas Turbines, 1998.

77. NFPA-77, Standard for the Inspection, Testing, and Maintenance of Water-Based Fire Protection Systems, 1998.

78. NFPA-72, National Fire Alarm Code, 1996.

79. 10 CFR 72 Certificate of Compliance 1014, Rev. 0, HI-STORM 100 System, May, 2000.

80. 10 CFR 71 Certificate of Compliance 9261, Rev. 0, HI-STAR 100 System, March, 1999.

81. NFPA 16A, Standard for the Installation of Closed-Head Foam-Water Sprinkler and Foam-Water Spray Systems, 1994.

82. NFPA 14, Standard for the Installation of Standpipe and Hose Systems, 1996.

83. NFPA 24, Standard for the Installation of Private Fire Service Mains and Their Appurtenances, 1995.

84. PFSF Calculation No. 05996.02 G(B)-11, Dynamic Settlements of the Soils Underlying the Site, Revision 1, Stone & Webster.

cask drop analysis for VSC-24 concurred that drops between 18 and 80 inches can be sustained with acceptable damage (i.e. without breaching the confinement boundary, preventing removal of fuel assemblies, causing a criticality accident, or causing a structural failure of the concrete cask so it can not maintain its shielding function).

Based on the engineering judgment, drops from heights up to 18 inches are not considered to be a concern. Since the TranStor cask and basket are similar to the VSC-24 and designed for the same drop loads, no additional analysis is required." The TranStor canister is analyzed and shown to withstand a vertical deceleration of 50 g, analyzed to result from vertical end drop of a TranStor shipping cask onto its impact limiters (Reference 5). SNC has performed additional calculations which indicate that stresses in the various canister components remain within code allowables, and the canister and its internals would continue to perform their safety functions, for a vertical deceleration of 124 g (Reference 23).

Cask Transporter Carrying a Storage Cask Loaded with Spent Fuel

In addition to the cask analyses, the following evaluation is provided to quantify the effects of natural forces on the transporter loaded with a cask full of spent fuel assemblies to show that a loaded transporter will not tip or overturn.

Information was reviewed from two track type cask transporters that have recently been supplied for similar casks to establish a basis for the cask transporter stability analysis, since the actual transporter to be used at the PFSF has not been determined. The transporters are manufactured by J&R Engineering and Lift Systems (References 72 and 73). The following information was collected:

Attribute	J&R Engineering 160 ton unit	Lift Systems 180 ton unit
Width of transporter	228 in.	228 in.
Length of transporter	336 in.	297 in.
Height of transporter (w/ cask)	264 in.	271 in.
Center of Gravity Height	55 in.	66 in.
Weight of transporter (w/o cask)	185,000 lbs.	160,000 lbs.

The transporter by Lift Systems will be used to evaluate the transporter stability since it has the same width, highest center of gravity, highest height, and lowest weight.

The following information regarding the storage casks was obtained from the HI-STORM and TranStor SARs (References 2 and 3):

Attribute	HI-STORM	TranStor
Height of storage cask	231 in.	223 in.
Diameter of storage cask	133 in.	136 in.
Center of Gravity Height	123 in.	114 in.
Weight of loaded storage cask	355,575 lbs.	307,600 lbs.

The TranStor storage cask will be used in the transporter stability analysis since it has considerable less weight to resist overturning and approximately the same height and diameter.

a. Stability of a Loaded Cask Transporter with Tornado Missile Impact

The tornado-generated missile loading specified in Table 3.6-1 used for this analysis is a 3990 lb. automobile traveling at a horizontal velocity of 134 ft/sec. This missile will produce the highest momentum for tipping the loaded cask transporter. The tornado missile is assumed to strike the transporter in the worse case direction, which is against the side where the transporter has the least width i.e., resistance to tipover. In addition, the automobile is placed at the top of the transporter for maximum tipping potential and it is assumed the transporter will not slide. The transporter loading conditions are shown on Figure 8.2-1.

It is also assumed that the transporter components will retain structural integrity during missile impact. In the event a component, such as the lift beam, fails, the cask will simply drop approximately 4" to the ground. The HI-STORM and TranStor storage casks are determined to be structurally sound for drops up to 11 inches and 18 inches respectively, as shown in Section 8.2.6.

The event can be thought of as two separate events. The first event is the collision, during which some of the kinetic energy of the missile is transferred to the cask/transporter system (target). How much of the energy is imparted to the target depends upon the nature of the collision. Not all of the missile energy can be transferred to the target, since this would violate the law of conservation of momentum. The energy not transferred to the target remains as kinetic energy of the rebounding missile and/or inelastic strain energy during crushing of the missile.

Two different types of collision will be considered. In Case 1, it will be assumed that all the momentum is transferred from the automobile to the transporter and some of the kinetic energy of the missile is transferred into tipping the transporter but the rest is lost in crushing the automobile, which has no velocity after impact. In Case 2, which assumes a perfectly elastic collision, no energy is lost and both momentum and kinetic energy are conserved during impact. Both cases were reviewed to determine which would cause the worst-case tipping.

Case 1 – Inelastic Collision (automobile doesn't rebound after the impact)

From the principles of conservation of momentum, the change in angular momentum of the missile due to the impact must equal the change in angular momentum of the loaded transporter. If the missile impact is applied at the top of the loaded transporter such that it pivots about a bottom corner point (P) then the angular momentum of the missile before impact relative to pivot point P is:

Angular momentum of the missile = $m_m V_o H$

where:

m_m = mass of missile = 3990 lbs. / 386 in/sec^2 = 10.34 lb-sec^2 / in.
V_o = initial velocity of missile = 134 fps = 1608 in/sec
H = height of transporter = 271 inches

Assuming all the angular momentum is imparted to the loaded transporter, the change in angular momentum of the loaded transporter about point P becomes:

Angular momentum of the transporter = $I_p \omega_p$

where:

I_p = mass moment of inertia of loaded transporter about pivot point P
ω_p = angular velocity of the transporter after impact

The mass moment of inertia of the cask about pivot point P is:

$$I_{p\,cask} = m_{cask}/12(3r_{cask}^2 + h_{cask}^2) + m_{cask}\, d_{cg\,cask}^2$$

where:

m_{cask} = mass of cask = 307,600 lbs / 386 in/sec^2 = 797 lb-sec^2 / in.
r_{cask} = radius of cask = 136 in./2 = 68 in.
h_{cask} = height of cask = 223 in.
$d_{cg\,cask}$ = distance from cask center of gravity to pivot point P calculated from the cask center of gravity height raised 4" (118") and the horizontal distance from the center of gravity to pivot point P (taken as half the transporter width, 228 in. /2 = 114) or $d_{cg\,cask} = [(118)^2 + (114)^2]^{1/2} = 164$ in.

Therefore, the cask mass moment of inertia about pivot point P is:

$$I_{p\,cask} = 797/12\,[3(68)^2 + (223)^2] + (797)(164)^2 = 25.66 \times 10^6 \text{ in·lb·sec}^2$$

The mass moment of inertia of the transporter about pivot point P is (assume the transporter is a rectangular parallelepiped that represents the lower "track" portion of the transporter where most of the weight is located):

$$I_{p\,xptr} = m_{xptr}/12\ (h_{xptr}^2 + w_{xptr}^2) + m_{xptr}\, d_{cg\,xptr}^2$$

where:

m_{xptr} = mass of transporter = 160,000 lbs / 386 in/sec^2 = 415 lb-sec^2/in.
h_{xptr} = height of transporter for calculating center of gravity (assume twice the height of the center of gravity) = 66 in. x 2 = 132 in.
w_{xptr} = overall width of transporter = 228 in.
$d_{cg\,xptr}$ = distance from transporter center of gravity to pivot point P calculated from the transporter center of gravity height (66") and the horizontal distance from the center of gravity to pivot point P (taken as half the transporter width, 228 in./2 = 114") or $d_{cg\,xptr} = [(66)^2 + (114)^2]^{1/2} = 132$ in.

Therefore, the transporter mass moment of inertia about pivot point P is:

$$I_{p\,xptr} = 415/12\ (132^2 + 228^2) + (415)(132)^2 = 9.63 \times 10^6 \text{ in}\cdot\text{lb}\cdot\text{sec}^2$$

The total mass moment of inertia of the loaded transporter about pivot point P then is:

$$\text{Total } I_p = 25.66 \times 10^6 + 9.63 \times 10^6 = 35.29 \times 10^6 \text{ in}\cdot\text{lb}\cdot\text{sec}^2$$

Equating the two angular momentums, the angular velocity (ω_p) of the loaded transporter about P following the impact is:

$$\omega_p = m_m V_o H / I_p = (10.34)(1608)(271) / (35.29\times10^6) = \underline{0.1277 \text{ rads/sec}}$$

Case 2 – Elastic Collision (automobile rebounds after the impact)

The impact is conservatively assumed to be totally elastic such that both momentum and energy are conserved during impact. The angular momentum and kinetic energy of the missile before and after the impact is:

Before impact: Angular momentum of the missile = $m_m V_o H$
Kinetic energy of the missile = $0.5\, m_m V_o^2$

After impact: Angular momentum of the missile = $m_m V_f H$
Kinetic energy of the missile = $0.5\, m_m V_f^2$

where:

m_m = mass of missile = 10.34 lb-sec^2 / in.
V_o = initial velocity of missile = 1608 in./sec
H = height of transporter = 271 inches
V_f = velocity of missile after impact

After impact the angular momentum of the transporter = $I_p\omega_p$

where:

I_p = mass moment of inertia of loaded transporter about pivot point P
= 35.29 x 10^6 in·lb·sec^2
ω_p = angular velocity of the transporter after impact

The kinetic energy of the cask after impact = 0.5 $I_p\, \omega_p^2$

Equating the angular momentum of the missile before impact to the total angular momentum after impact,

$$m_m V_o H = m_m V_f H + I_p \omega_p$$

Equating the kinetic energy before impact to the total kinetic energy after impact,

$$0.5\, m_m V_o^2 = 0.5\, m_m V_f^2 + 0.5\, I_p\, \omega_p^2$$

Substituting the values of m_m, V_o, H and I_p, and solving for V_f and ω_p,

V_f = -1540 ft/sec (missile rebound velocity)

ω_p = $\underline{0.250 \text{ rad/sec}}$

Case 2, with the higher angular velocity of 0.250 rad/sec, will cause the worst-case tipping of the loaded transporter.

The second part of the event consists of motion of the target after impact. Immediately after impact, the target is in it's original position and starts to rotate about the pivot point P with an angular velocity of 0.250 rad/sec. The weight of the cask/transporter creates a moment (torque) about the pivot point, which opposes the motion and decelerates the target. This moment reduces the angular velocity until it reaches zero, and then gravity

returns the target to it's original position. The distance the center of gravity moves upward before stopping can be calculated by equating the rotational kinetic energy of the target to the work required to raise the center of gravity.

The rotational kinetic energy of the target after impact can be determined and as the loaded transporter tips about point P, the kinetic energy is transferred to potential energy as the center of gravity rises a distance y:

$$
\begin{aligned}
E_{tipping} &= \text{Kinetic Energy} = \text{Increase in Potential Energy} \\
&= 0.5\, I_p\, \omega_p^2 = W_t\, y \\
&= 0.5(35.29 \times 10^6)(0.250)^2 = 467{,}600\, y \\
y &= \underline{2.36 \text{ in.}}
\end{aligned}
$$

In conclusion, 1) The loaded transporter will not tip over because the center of gravity only lifts 2.36", which is considerably less than 51.6", the distance required for the center of gravity to pass over the pivot point P and 2) The Technical Specification lift height won't be exceeded since raising the cask an additional 2.36" above the carrying height of 4" = 6.36", which is less than the 10" allowable lift height.

b. Stability of a Loaded Cask Transporter Under Seismic Conditions

The transporter is not designated an important to safety component and therefore is not subject to specific seismic design requirements. However, this section provides the necessary evaluation based on the PFSF design basis ground motion peak ground acceleration ensuring that the loaded transporter will not tip due to seismic loading.

The loaded transporter is generally a flexible system with low frequencies, which would probably not be excited due to the short duration of a seismic event. In the event a seismic load could cause a failure of the transporter structure, the cask would drop or lower to the ground as vehicle members fail or yield. In the event that the cask were to drop, the HI-STORM and TranStor storage casks are determined to be structurally

sound for drops up to 11 inches and 18 inches respectively, as shown in Section 8.2.6.2. Since the transporter is rectangular in shape, consider an earthquake in the worse case direction, which is perpendicular to the width of the transporter. In order for the loaded transporter to tip or overturn, the moments caused by the earthquake accelerations must exceed the resisting moment due to the loaded transporter weight. Calculating the moments about pivot point P then:

$$M_{p\,eq} = g\,W_t\,v_{cg} + g\,W_t\,h_{cg}$$
$$M_{p\,resist} = W_t\,h_{cg}$$

where:

- g = design earthquake acceleration = 0.53g (horizontal & vertical)
- W_t = total weight of cask & transporter = 307,600 lbs. (cask) + 160,000 lbs. (cask transporter) = 467,600 lbs.
- h_{cg} = horizontal distance from center of gravity of a loaded transporter to pivot point P (half the transporter width) = 228 in./2 = 114 in.
- v_{cg} = vertical distance from center of gravity of a loaded transporter to the ground = combination of the cask center of gravity height when the cask is raised 4 in. above the ground and the transporter center of gravity height or

$$v_{cg} = [(cask_{cg} + 4\text{ in.})\,W_{cask} + (transporter_{cg})\,W_{xptr}\,] / W_t$$

$$v_{cg} = [(114 + 4)\,307{,}600 + (66)\,160{,}000] / 467{,}600 = 100\text{ in.}$$

Therefore, the moments are:

$$M_{p\,eq} = (0.53)(467{,}600)(100) + (0.53)(467{,}600)(114) = \underline{53{,}035{,}192\text{ in}\cdot\text{lbs}}$$

$$M_{p\,resist} = (467{,}600)(114) = \underline{53{,}306{,}400\text{ in}\cdot\text{lbs}}$$

Since the moment due to the earthquake acceleration is less than the moment due to the loaded transporter weight, the loaded transporter will not tip or overturn as a result of the design basis ground motion.

However, the difference in moments is slight. If the storage cask is carried higher than 4 in. off the ground as allowed by the storage system Technical Specifications, thus

raising the loaded transporter center of gravity, it is possible that the moment due to the earthquake could exceed the resisting moment and the transporter could begin to tip. Therefore, to preclude any incipient tipping, the specification to purchase the transporter for PFSF will include requirements to analyze any proposed transporter design to ensure that its dimensions, center of gravity, and weight when carrying a loaded storage cask are such that the loaded transporter will not begin to tip due to the PFSF design basis ground motion.

8.2.6.3 Accident Dose Calculations

Based on the results of the analyses described above, the cask/canister storage systems would retain their confinement integrity and there would be no release of radioactivity and no resultant doses in the event of hypothetical drop/tipover of a fully loaded storage cask. For tipover of a HI-STORM storage cask, it is considered that localized damage to the radial concrete shield and outer steel shell where the cask impacts the pad could result in an increased surface dose rate due to the damage. However, this would not produce a noticeable increase in the dose rates at the RA fence or OCA boundary because the affected area would likely be small (HI-STORM SAR, Section 11.2.3). The maximum concrete crush depth of 2 inches calculated for the TranStor storage cask would approximately double the dose rates in the localized area, but would not significantly affect the overall dose rates from the storage cask (TranStor SAR Section 11.2.10).

In the hypothetical event of a storage cask tipover / drop accident that is postulated to result in damage to a storage cask, the PFSF staff would evaluate the extent of damage and if needed would remove a canister from the damaged storage cask and transfer the canister to a new storage cask in the Canister Transfer Building utilizing a transfer cask to provide canister shielding and a single-failure-proof crane.

8.2.7 Canister Leakage Under Hypothetical Accident Conditions

The leakage of a canister under hypothetical accident conditions wherein cladding of 100% of the fuel rods is postulated to have ruptured is classified as Design Event IV as defined by ANSI/ANS-57.9. This is not a credible accident at the PFSF.

8.2.7.1 Cause of Accident

The HI-STORM and TranStor canisters are totally sealed, integrally welded pressure vessels, designed to Section III of the ASME BPVC. There are no gaskets, mechanical seals, or packing that could provide a potential leakage path for the radioactive fission products contained within the fuel cladding. The canisters are provided with multiple closures to confine the radioactive fuel. Following welding of the closures, the canisters are tested to verify their leaktight integrity. No components are required to penetrate the sealed canisters after helium backfilling is completed and the outer closure is welded in place. The postulated failure of the cladding of all fuel rods in a canister and release of gases normally contained in the fuel rod cladding under pressure would not challenge the integrity of the canisters (Section 8.2.10). Maximum canister leakage under conditions wherein cladding of 100% of the fuel rods is postulated to have ruptured is considered to be a non-credible event, which will not occur over the life of the PFSF. Nevertheless, this accident is hypothesized and analyzed below. Doses resulting from the canister leakage under hypothetical accident conditions were calculated in accordance with Interim Staff Guidance-5 (ISG-5, Reference 31).

8.2.7.2 Accident Analysis

In this accident analysis, it is postulated that a canister leaks at the maximum rate permitted by the closure helium leakage test acceptance criteria. Such a leak would require a significant defect in each of two redundant closure welds. In this hypothetical

TORNADO MISSILE LOADS

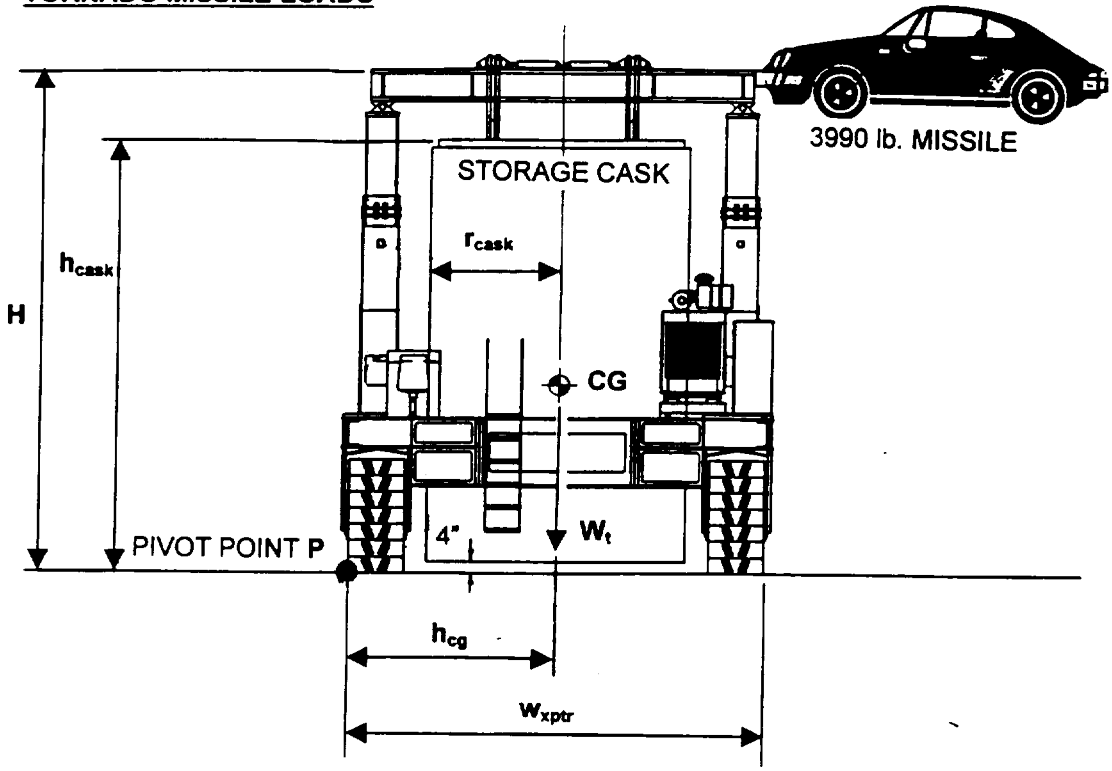

EARTHQUAKE LOADS

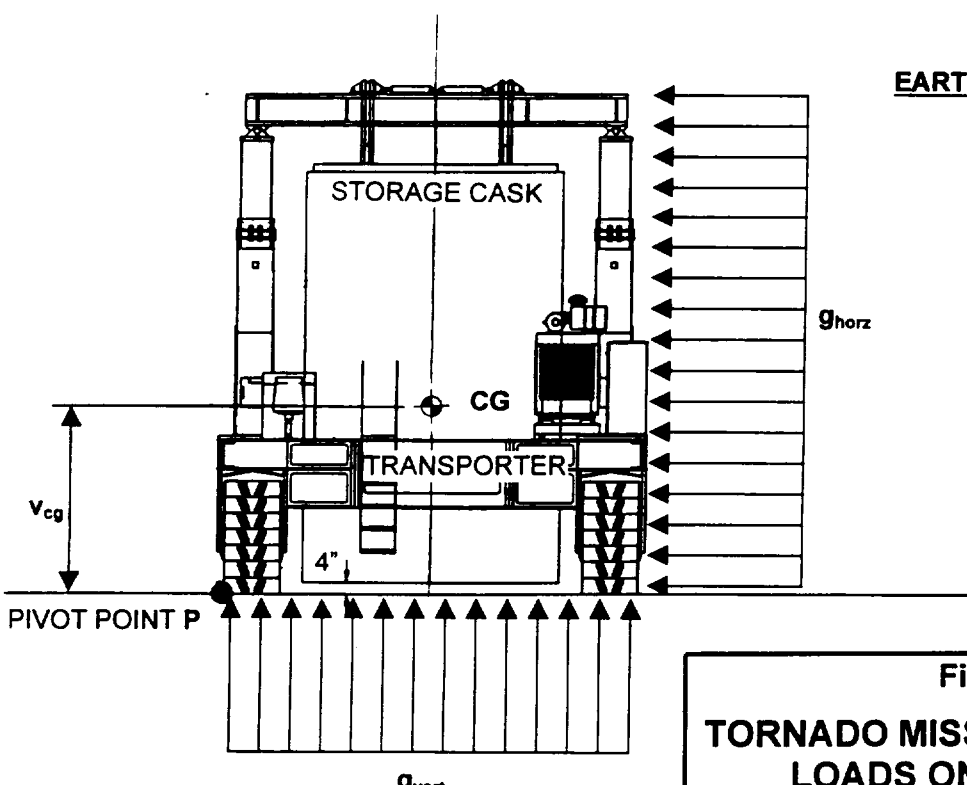

Figure 8.2-1

TORNADO MISSILE / EARTHQUAKE LOADS ON TRANSPORTER

PRIVATE FUEL STORAGE FACILITY
SAFETY ANALYSIS REPORT

DOCUMENT CONTROL

PAGE	REVISION
Document Control Tab	
a	10
b	10
c	10
d	10
e	10
f	10
g	10
h	10
i	10
j	10
k	10
l	10
m	10
n	10
o	10
p	10
q	10
r	10
Table of Contents Tab	
i	0
ii	6
iii	8
iv	3
Chapter 1 Tab	
1-i	0
1-ii	0
1.1-1	1
1.1-2	0
1.2-1	1
1.2-2	6
1.2-3	6
1.2-4	6
1.2-5	6
1.2-6	6
1.2-7	6
1.2-8	6
1.2-9	6
1.2-10	6
1.3-1	1
1.3-2	9
1.4-1	6

DOCUMENT CONTROL

PAGE	REVISION
1.4-2	0
Chapter 2 Tab	
2-i	6
2-ii	6
2-iii	2
2-iv	7
2-v	6
2-vi	0
2-vii	2
2-viii	6
2-ix	6
2-x	6
2-xi	5
2-xii	5
2.1-1	0
2.1-2	1
2.1-3	7
2.1-4	7
2.2-1	0
2.2-2	2
2.2-3	6
2.2-4	6
2.2-5	6
2.2-6	6
2.2-7	6
2.2-8	6
2.2-9	6
2.2-10	6
2.3-1	2
2.3-2	6
2.3-2a	6
2.3-2b	6
2.3-3	1
2.3-4	1
2.3-5	1
2.3-6	1
2.3-7	1
2.3-8	6
2.3-9	6
2.3-10	6
2.3-11	6
2.3-11a	6
2.3-11b	6

DOCUMENT CONTROL

PAGE	REVISION
2.3-12	1
2.3-13	1
2.3-14	1
2.3-15	1
2.3-16	1
2.3-17	1
2.3-18	5
2.3-19	1
2.3-20	1
2.3-21	1
2.3-22	1
2.3-23	1
2.3-24	6
2.3-25	6
2.3-26	6
2.3-27	6
2.3-28	6
2.3-29	1
2.3-30	1
2.3-31	6
2.3-32	6
2.3-33	6
2.3-34	6
2.3-35	6
2.3-36	6
2.3-37	6
2.3-38	6
2.4-1	0
2.4-2	0
2.4-3	0
2.4-4	0
2.4-5	0
2.4-6	0
2.4-7	0
2.4-8	0
2.4-9	1
2.4-10	1
2.4-11	0
2.4-12	2
2.4-13	8
2.4-14	8
2.4-15	8
2.4-16	2
2.4-17	6

DOCUMENT CONTROL

PAGE	REVISION
2.4-18	6
2.5-1	0
2.5-2	1
2.5-3	2
2.5-4	2
2.5-5	2
2.5-6	2
2.5-7	2
2.5-8	2
2.5-9	2
2.5-10	2
2.5-11	2
2.5-12	10
2.6-1	2
2.6-2	4
2.6-3	2
2.6-4	2
2.6-5	2
2.6-6	2
2.6-7	2
2.6-8	2
2.6-9	2
2.6-10	6
2.6-11	2
2.6-12	7
2.6-13	10
2.6-14	6
2.6-15	7
2.6-16	9
2.6-17	9
2.6.17a	9
2.6.17b	7
2.6-18	6
2.6-19	5
2.6-20	5
2.6-21	5
2.6-22	5
2.6-23	5
2.6-24	5
2.6.25	5
2.6.26	5
2.6-27	5
2.6-28	5
2.6-29	7

DOCUMENT CONTROL

PAGE	REVISION
2.6-30	7
2.6-31	7
2.6-32	7
2.7-1	6
2.7-2	6
2.7-3	6
2.7-4	6
2.7-5	6
2.7-6	6
2.7-7	6
2.7-8	6
2.7-9	6
2.7-10	6
2.7-11	6
2.7-12	6
2.7-13	6
2.7-14	6
2.7-15	6
2.7-16	6
2.7-17	6
2.7-18	6
2.8-1	7
2.8-2	6
2.8-3	6
2.8-4	6
2.8-5	6
2.8-6	6
2.9-1	6
2.9-2	6
2.9-3	6
2.9-4	6
2.9-5	6
2.9-6	6
2.10-1	7
2.10-2	6
2.10-3	6
2.10-4	6
2.11-1	0
2.11-2	6
2.11-3	6
2.11-4	6
2.11-5	6
2.11-6	6
2.11-7	6

DOCUMENT CONTROL

PAGE	REVISION
2.11-8	6
2.11-9	6
2.11-10	9
2.11-11	9
2.11-12	6
Table 2.2-1	0
Table 2.3-1	0
Table 2.3-2 (1 of 5)	2
Table 2.3-2 (2 of 5)	2
Table 2.3-2 (3 of 5)	2
Table 2.3-2 (4 of 5)	2
Table 2.3-2 (5 of 5)	1
Table 2.3-3	1
Table 2.4-1	0
Table 2.4-2	0
Table 2.4-3	2
Table 2.4-4	8
Table 2.4-5	2
Table 2.4-6	2
Table 2.4-7	2
Table 2.4-8	2
Table 2.4-9	2
Table 2.4-10	2
Table 2.4-11 (1 of 2)	6
Table 2.4-11 (2 of 2)	6
Table 2.4-12 (1 of 8)	6
Table 2.4-12 (2 of 8)	6
Table 2.4-12 (3 of 8)	6
Table 2.4-12 (4 of 8	6
Table 2.4-12 (5 of 8)	6
Table 2.4-12 (6 of 8)	6
Table 2.4-12 (7 of 8)	6
Table 2.4-12 (8 of 8)	6
Table 2.6-1A	5
Table 2.6-1B	5
Table 2.6-1C	5
Table 2.6-2 (1 of 14)	0
Table 2.6-2 (2 of 14)	0
Table 2.6-2 (3 of 14)	0
Table 2.6-2 (4 of 14)	0
Table 2.6-2 (5 of 14)	0
Table 2.6-2 (6 of 14)	0
Table 2.6-2 (7 of 14)	0
Table 2.6-2 (8 of 14)	0

DOCUMENT CONTROL

PAGE	REVISION
Table 2.6-2 (9 of 14)	0
Table 2.6-2 (10 of 14)	0
Table 2.6-2 (11 of 14)	0
Table 2.6-2 (12 of 14)	0
Table 2.6-2 (13 of 14)	0
Table 2.6-2 (14 of 14)	0
Table 2.7-1	0
Table 2.7-2	0
Table 2.7-3	0
Table 2.8-1 (1 of 3)	1
Table 2.8-1 (2 of 3)	1
Table 2.8-1 (3 of 3)	1
Table 2.8-2	6
Figure 2.1-1	2
Figure 2.1-2 (1 of 2)	2
Figure 2.1-2 (2 of 2)	0
Figure 2.2-1	0
Figure 2.2-2	0
Figure 2.2-3	0
Figure 2.2-4	0
Figure 2.3-1	0
Figure 2.3-2	0
Figure 2.3-3	0
Figure 2.3-4	0
Figure 2.3-5	0
Figure 2.3-6	0
Figure 2.3-7	0
Figure 2.3-8	0
Figure 2.3-9	0
Figure 2.3-10	0
Figure 2.3-11	0
Figure 2.3-12	0
Figure 2.3-13	6
Figure 2.3-14	6
Figure 2.3-15	6
Figure 2.4-1	0
Figure 2.4-2	0
Figure 2.4-3	0
Figure 2.4-4	0
Figure 2.4-5	0
Figure 2.5-1	2
Figure 2.5-2	2
Figure 2.6-1	0
Figure 2.6-2 (1 of 2)	5

DOCUMENT CONTROL

PAGE	REVISION
Figure 2.6-2 (2 of 2)	0
Figure 2.6-3	0
Figure 2.6-4	0
Figure 2.6-5	0
Figure 2.6-6	0
Figure 2.6-7A	5
Figure 2.6-7B	5
Figure 2.6-7C	5
Figure 2.6-8A	5
Figure 2.6-8B	5
Figure 2.6-8C	5
Figure 2.6-9	0
Figure 2.6-10	0
Figure 2.6-11	5
Figure 2.6-12	5
Appendix 2A Tab	
Utah Land Cover Types	0
Appendix 2B Tab	
Life History Information	1
Appendix 2C Tab	
Relative Biological Value of Land Cover Types for Wildlife Species	0
Appendix 2D Tab	
Vegetation-Soil Site Type Inventory	0
Chapter 3 Tab	
3-i	6
3-ii	2
3.1-1	2
3.1-2	6
3.1-3	6
3.1-4	0
3.2-1	2
3.2-2	9
3.2-3	2
3.2-4	6
3.2-5	9
3.2-6	7
3.2-7	7
3.2-8	1

DOCUMENT CONTROL

PAGE	REVISION
3.3-1	0
3.3-2	0
3.3-3	2
3.3-4	1
3.3-5	1
3.3-6	6
3.3-7	6
3.3-8	6
3.3-9	6
3.3-10	6
3.3-11	6
3.3-12	6
3.4-1	0
3.4-2	1
3.5-1	8
3.5-2	0
Figure 3.1-1	2
Figure 3.1-2	0
Figure 3.1-3	0
Figure 3.1-4	0
Figure 3.1-5	1
Figure 3.2-1 (1 of 2)	1
Figure 3.2-1 (2 of 2)	1
Figure 3.2-2 (1 of 4)	2
Figure 3.2-2 (2 of 4)	2
Figure 3.2-2 (3 of 4)	2
Figure 3.2-2 (4 of 4)	2
Figure 3.3-1	8
Figure 3.3-2	0
Figure 3.3-3	0
Figure 3.3-4	0
Chapter 4 Tab	
4-i	7
4-ii	6
4-iii	7
4-iv	6
4-v	6
4-vi	6
4-vii	7
4-viii	6
4-ix	7
4-x	7
4.1-1	2

DOCUMENT CONTROL

PAGE	REVISION
4.1-2	6
4.1-3	6
4.1-4	6
4.1-5	6
4.1-6	6
4.1-7	6
4.1-8	6
4.1-9	10
4.1-10	6
4.1-11	10
4.1-12	6
4.1-13	7
4.1-13a	7
4.1-13b	7
4.1-13c	7
4.1-13d	7
4.1-14	6
4.1-15	6
4.1-16	6
4.1-17	6
4.1-18	6
4.1-19	6
4.1-20	6
4.1-21	6
4.1-22	6
4.1-23	6
4.1-24	7
4.1-25	8
4.1-26	8
4.2-1	0
4.2-2	6
4.2-3	8
4.2-4	6
4.2-5	8
4.2-6	6
4.2-7	7
4.2-7a	7
4.2-7b	7
4.2-8	6
4.2-9	8
4.2-10	6
4.2-11	6
4.2-12	6
4.2-13	6

DOCUMENT CONTROL

PAGE	REVISION
4.2-14	6
4.2-15	6
4.2-16	8
4.2-17	8
4.2-18	8
4.2-19	8
4.2-20	6
4.2-21	6
4.2-22	8
4.2-23	6
4.2-24	6
4.2-25	6
4.3-1	2
4.3-2	6
4.3-3	6
4.3-4	6
4.3-5	6
4.3-6	6
4.3-7	6
4.3-8	6
4.3-9	7
4.3-9a	7
4.3-9b	7
4.3-10	6
4.3-11	8
4.3-12	6
4.3-13	6
4.3-14	6
4.3-15	6
4.3-16	6
4.4-1	2
4.4-2	2
4.4-3	6
4.4-4	6
4.4-5	6
4.4-6	6
4.4-7	6
4.4-8	6
4.4-9	7
4.4-9a	7
4.4-9b	7
4.4-10	8
4.4-11	6
4.4.12	6

DOCUMENT CONTROL

PAGE	REVISION
4.4.13	6
4.4.14	6
4.4-15	6
4.4-16	6
4.5-1	9
4.5-2	6
4.5-3	6
4.5-4	6
4.5-5	6
4.5-6	6
4.5-7	6
4.5-8	6
4.5-9	6
4.5-10	6
4.6-1	0
4.6-2	6
4.6-3	9
4.6-4	0
4.7-1	0
4.7-2	0
4.7-3	0
4.7-4	1
4.7-5	2
4.7-6	1
4.7-7	1
4.7-8	1
4.7-9	6
4.7-10	6
4.7-11	6
4.7-12	6
4.7-13	6
4.7-14	6
4.7-15	6
4.7-16	6
4.7-17	6
4.7-18	6
4.7-19	6
4.7-20	6
4.8-1	6
4.8-2	6
4.8-3	7
4.8-4	7
4.8-5	7
4.8-6	6

DOCUMENT CONTROL

PAGE	REVISION
Table 4.1-1	0
Table 4.1-2	0
Table 4.1-3 (1 of 2)	6
Table 4.1-3 (2 of 2)	6
Table 4.1-4	6
Table 4.1-5	6
Table 4.1-6 (1 of 2)	7
Table 4.1-6 (2 of 2)	6
Table 4.1-7	8
Table 4.2-1	8
Table 4.3-1	6
Table 4.4-1	6
Table 4.7-1	6
Table 4.7-2	6
Figure 4.4-1	7
Appendix 4A	
Artist's Concepts of the PFSF, Intermodal Transfer Point, and the Low Corridor Rail Line/Sidings	7
Chapter 5 Tab	
5-i	2
5-ii	0
5.1-1	0
5.1-2	2
5.1-3	7
5.1-4	2
5.1-5	2
5.1-6	2
5.1-7	2
5.1-8	2
5.2-1	0
5.2-2	0
5.2-3	0
5.2-4	0
5.3-1	3
5.3-2	0
Chapter 6 Tab	
6-i	0
6-ii	0
6-iii	0
6-iv	0

DOCUMENT CONTROL

PAGE	REVISION
6.1-1	0
6.1-2	0
6.1-3	0
6.1-4	6
6.1-5	6
6.1-6	6
6.2-1	6
6.2-2	6
6.3-1	6
6.3-2	0
Table 6.1-1	0
Table 6.1-2 (sht 1 of 4)	3
Table 6.1-2 (sht 2 of 4)	3
Table 6.1-2 (sht 3 of 4)	3
Table 6.1-2 (sht 4 of 4)	3
Figure 6.1-1	0
Chapter 7 Tab	
7-i	7
7-ii	7
7-iii	6
7-iv	7
7.1-1	7
7.1-2	0
7.2-1	0
7.2-2	7
7.2-3	7
7.2-4	8
7.2-5	7
7.2-6	7
7.2-7	7
7.2-8	7
7.3-1	7
7.3-2	7
7.4-1	7
7.4-2	7
7.5-1	7
7.5-2	7
Table 7.3-1	8
Figure 7.2-1	0
Appendix 7A	
Basis for the Use of a 3.8% Discount Rate	7

DOCUMENT CONTROL

PAGE	REVISION
Appendix 7B	
At-Reactor Spent Fuel Storage Cost Summaries	8
Appendix 7C	
Summary of Avoided Costs (PFS Net Benefits)	8
Appendix 7D	
Basis for Using Spent Fuel Pool Storage Costs Following Shutdown And Prior to Decommissioning	7
Chapter 8 Tab	
8-i	7
8-ii	6
8-iii	3
8-iv	3
8-v	3
8-vi	3
8.1-1	0
8.1-2	1
8.1-3	0
8.1-4	7
8.1-5	7
8.1-6	7
8.1-7	7
8.1-8	7
8.1-9	7
8.1-9a	7
8.1-9b	7
8.1-9c	7
8.1-9d	7
8.1-9e	7
8.1-9f	7
8.1-10	6
8.1-11	6
8.1-12	6
8.1-13	6
8.1-14	6
8.1-15	7
8.1-16	7
8.2-1	0
8.2-2	0
8.2-3	0
8.2-4	0
8.2-5	0

DOCUMENT CONTROL

PAGE	REVISION
8.2-6	1
8.2-7	0
8.2-8	0
8.2-9	0
8.2-10	0
8.2-11	0
8.2-12	0
8.2-13	1
8.2-14	0
8.2-15	0
8.2-16	0
8.2-17	0
8.2-18	0
8.2-19	0
8.2-20	0
8.2-21	0
8.2-22	0
8.3-1	6
8.3-2	6
8.3-3	7
8.3-4	7
8.3-5	7
8.3-6	7
8.3-7	7
8.3-8	7
8.3-9	7
8.3-10	7
8.4-1	6
8.4-2	6
Table 8.1-1	3
Table 8.1-1A	3
Table 8.1-2 (1 of 5)	2
Table 8.1-2 (2 of 5)	0
Table 8.1-2 (3 of 5)	0
Table 8.1-2 (4 of 5)	0
Table 8.1-2 (5 of 5)	0
Table 8.1-3	0
Table 8.2-1	1
Figure 8.1-1	0
Figure 8.1-2	0
Figure 8.2-1	0
Figure 8.2-2	0
Figure 8.2-3	0
Figure 8.2-4	0

DOCUMENT CONTROL

PAGE	REVISION
Figure 8.2-5	0
Figure 8.2-6	0
Figure 8.2-7	0
Figure 8.2-8	0
Figure 8.2-9	0
Figure 8.2-10	0
Figure 8.2-11	0
Figure 8.2-12	0
Figure 8.2-13	0
Figure 8.2-14	0
Appendix 8A Tab	
PFSF Fuel Storage Site Proposal Initial Screening; Answers to Screening Questions	3
Appendix 8B Tab	
Private Fuel Storage Project Potential Host Community Description and Background	3
Appendix 8C Tab	
Response to Site Selection Questionnaire	3
Chapter 9 Tab	
9-i	7
9-ii	0
9-iii	7
9-iv	7
9.1-1	9
9.1-2	7
9.1-3	7
9.1-4	2
9.1-5	7
9.1-6	7
9.1-7	7
9.1-8	7
9.1-9	7
9.1-10	8
9.1-11	7
9.1-12	7
9.2-1	9
9.2-2	7
9.2-3	9
9.2-4	7
9.3-1	7
9.3-2	0

DOCUMENT CONTROL

PAGE	REVISION
9.4-1	7
9.4-2	0
9.5-1	7
9.5-2	0
9.6-1	2
9.6-2	7
9.6-3	2
9.6-4	1
Table 9.1-1 (1 of 4)	7
Table 9.1-1 (2 of 4)	7
Table 9.1-1 (3 of 4)	7
Table 9.1-1 (4 of 4)	7

700 to about 900 mg/l with a few isolated wells above 1,000 mg/l TDS. A well south of the Skull Valley Indian Reservation yielded a TDS concentration of greater than 2,500 mg/l (Arabasz et al., 1987). Sodium and chloride are the major ions found in these waters.

Toward the center part of the valley, away from the alluvial apron, unconsolidated lacustrine materials are interstratified with clastic material. Wells in this area tend to have lower yields and poorer quality water (TDS >1,000 mg/l) and are used mainly for irrigation and stock watering. The north end of the valley has generally high TDS concentrations, in the range of 1,600 to 7,900 mg/l with sodium and chloride again being the main constituents (Arabasz et al., 1987).

Based on boring data obtained at the PFSF site, the uppermost soil layer consists of interbedded silt, silty clay, and clayey silt with a thickness of approximately 30 ft. This layer is underlain by very dense fine sand and silt. The groundwater table was encountered in the borings at a depth of 125 ft (approximate elevation 4,350 ft).

Limited hydraulic characteristics of the soil in the PFSF vicinity are available from the on-site boring program (SWEC, 1999b).

The hydraulic gradient was estimated to be approximately 9.5×10^{-4}. (Hood and Waddell, 1968). Groundwater flows in a south to north direction toward the Great Salt Lake.

Soil interpretations prepared by USDA (undated) indicate that the permeability of a silt soil in Skull Valley ranges from 0.2 to 0.6 inch/hr. The average groundwater velocity was estimated to be approximately 2.8×10^{-3} to 8.5×10^{-3} gallons/day/sq ft.

The source of groundwater flow at the PFSF is mainly derived from precipitation that falls at the higher elevations of the Stansbury and Cedar Mountains. As a result of the low permeability deposits and high evapotranspiration at the PFSF, rainfall at the PFSF is unlikely to contribute to groundwater flow.

Initial testing of the onsite groundwater monitoring well indicates that development of the PFSF will have no measurable offsite effects on existing groundwater quality or levels of a water supply well at the site (SWEC, 1999b).

2.5.6 Contaminant Transport Analysis

The nature and form of the material stored (spent fuel rod assemblies) and the method of storage (dry casks) preclude the possibility of a liquid contaminant spill. Discussion of potential contamination of groundwater is not applicable.

locations of these CPTs and DMTs are presented in Figure 2.6-12. The results from this investigation are presented in ConeTec (1999). The primary goal of this investigation was to develop profiles of the relative strength and compressibility of the soils within the depth interval of 10 ft to ~25 ft in the pad emplacement area. As stated in ConeTec (1999), the other interpretations are presented only as a guide for geotechnical use and should be carefully scrutinized for consideration in any geotechnical design.

This program included performing cone penetration tests (CPT) to develop continuous profiles of the strength of the soils in the upper layer (from the surface down to ~25 ft) within the pad emplacement area. It also included performing dilatometer tests (DMT) to develop profiles of the compressibility of the in situ soils. These were located, primarily, in areas where the tip resistance profiles from the CPT tests indicated that the in situ soils had the lowest strengths and the highest compressibilities.

Based on these borings and laboratory test data, the generalized subsurface profile consists of three layers, as shown in Figure 2.6-5. The uppermost layer extends to a depth of between 25 and 35 ft below existing grade and is mainly interlayered silt, silty clay, and clayey silt. SPT N-values for this layer are mostly between 8 and 20 blows per ft, with an average value of 16 blows per ft and a median value of 14 blows per ft, indicating that these are "stiff" or "medium dense" materials. The upper layer was subdivided based on the results of the cone penetration tests. More detailed stratigraphy is presented in the foundation profiles included in the SAR as Figure 2.6-5, Sheets 1 through 14. SAR Figure 2.6-19 identifies the locations of these foundation profiles in plan view.

There are some differences between the results of the borings and the CPTs in regard to describing the types of soils encountered, mostly in the 10 to 20 ft depth range. The

cone penetration testing program indicated that the soils between approximately 10 ft and 20 ft below existing grade at the site behave as though they are silty sands and sands. This finding was not corroborated by the descriptions of the soils obtained from that zone in the borings, many of which are supported by laboratory test results. As discussed in Section 2.6.1.6 of the SAR, to more accurately reflect the actual soil classification at the site, the SBT values reported by ConeTec (1999) were adjusted downward by 1 zone for those whose SBT values were greater than 5. Based on the results of this recalibration, the soil behavior type data from ConeTec (1999) are replotted, as shown in SAR Figure 2.6-5, Sheets 2 through 14, along with the data from the soil borings, to generate the foundation profiles at the pad emplacement area.

This layer is underlain by 25 to 30 ft of very dense, dry, fine sand with occasional thin layers of fine gravel and coarse sand. SPT N-values often are greater than 100 blows per 6 inches. A few clayey zones were encountered, but they had no apparent effect on the blow counts. The borings that were drilled to depths greater that 100 ft (Borings A-1, D-4, CTB-1, and CTB-5) indicate that this second layer of dense, dry, fine sand is underlain by very dense silt, silty sand, and sandy silt with occasional layers of clayey silt.

The groundwater table was encountered in Boring CTB-5(OW) at a depth of 125 ft in the area of the Canister Transfer Building. Seismic refraction results indicate the compression wave (P-wave) velocity (PFSF SAR, Appendix 2B) changes from approximately 2,800 fps to approximately 5,525 fps at about 100 to 130 ft depth, which corroborates the depth to the water table measured in Boring CTB-5(OW).

Borings AR-1 through AR-5 were drilled along the corridor for the access road, which extends easterly from the PFSF in the vicinity of the Administration Building to Skull Valley Road. These borings indicate that the near-surface soils are similar to the

by employing routine washing of trucks. Dust emissions from anticipated concrete batch plant operations will also be mitigated through the use of enclosures, hoods, shrouds, and water sprays. Gaseous emissions from construction equipment are mitigated typically by requiring regular maintenance of equipment.

Communications with local a supplier indicates that the estimated quantity of asphalt paving to be placed at the facility does not justify locating a batch plant onsite.

Construction related pollutant emissions cannot be well defined until such time as the construction process is broken down into its component operations and planned in some detail. However, estimates of air pollutant emissions due to construction activities are provided in Table 4.1-4 on the basis of estimated material usage (e.g., cubic yards of concrete) and reasonable assumptions regarding construction vehicle mileage and hours of operation during the construction phase. Emissions estimates are provided for fugitive dust emissions (PM10) from clearing and excavation activities as well as from the concrete batch plant. Gaseous criteria pollutant emissions (SO_2, NO_x, CO, VOC) from vehicular traffic (NO_x, CO, and VOC) are also provided. All of the construction activities are conservatively assumed to be occurring simultaneously during any given construction month for purposes of these emissions estimates. The emission factors used in the estimates for construction activities are taken from the 5th edition of EPA's AP-42 document (EPA 1995a) assuming reasonable levels of emissions control as needed to satisfy DEQ requirements. Vehicle emissions are derived from the latest version of EPA's MOBILE5b emissions estimating model (EPA 1996).

The plant wide controlled PM-10 emission factor (E) for concrete batching is taken from Section 11.12, Table 11.12-3 of AP-42 and is expressed as 0.12 pound per cubic yard of concrete produced. It is assumed that 125,300 cubic yards of concrete are produced in one year yielding 7.5 tons of PM-10 emissions per year or 0.6 ton per month.

The potential impact of these construction related pollutant emissions on ambient concentrations in public areas has also been assessed using the EPA

SCREEN3 screening level dispersion model (EPA 1995b). This model calculates ground level concentrations of pollutants emitted from both point and area sources as a function of downwind distance utilizing either a standard matrix of meteorological conditions designed to produce worst case impacts or user input meteorological conditions. For fugitive dust impact estimates, the neutral atmospheric stability class (D stability) and a wind speed of 5 meters per second is assumed to be a representative combination of conditions causing dusting. General construction activities such as excavation and other fugitive dust sources are represented as area sources while emissions from the concrete batch plant are treated as a point source. Ambient pollutant concentrations are calculated at two locations where the general public could be impacted: the closest point from the facility to Skull Valley Road; and at the Goshute Village, located approximately 3.5 miles from the site.

Based on estimated quantities of required concrete and information from local concrete suppliers, the concrete batch plant would be sized for a maximum capacity of 75 yd^3 per hour. The batch plant and material storage for this capacity would require a footprint area of approximately 300-ft. x 300-ft., or approximately 2 acres. The specific location for the batch plant on the PFSF site would be determined during the construction planning phase of the project, but it will likely be sited North of the Canister Transfer Building on the Eastern side of the storage area. The batch plant location would be provided with controls, e.g., perimeter berm and drainage retention, to mitigate any environmental effects on the immediate area.

Emissions from the concrete batch plant are treated as point sources. One-hour concentrations calculated by SCREEN3 are adjusted to 3-, 8-, and 24-hour average concentrations using the factors 0.9, 0.7, and 0.4, respectively. The annual average adjustment factor used is 0.05.

The concrete batch plant PM-10 emissions are assumed to be released from a height of 20 feet above ground level. Annual pollutant emissions are based on an assumed 2,200 hours per year of operation of the concrete batch plant.

The results of the screening level impact analysis are presented in Table 4.1-5 and indicate that the estimated pollutant concentrations at Skull Valley Road and at the nearest residences are all below the ambient air quality standards.

4.1.4 Effects on Hydrological Resources

There are no perennial streams at or near the PFSF and its access road. Several dry washes, which may flow for brief periods during spring snowmelt or local thunderstorms, will be crossed by the access road. Culverts will be provided through the access road embankment to carry the occasional runoff. Culverts will be sized to pass the 100-year flood for this area. Therefore, there will be no impact on area hydrology due to construction of the facility and its access road.

4.1.5 Effects on Mineral Resources

To assess the mineral potential of Skull Valley, PFS conducted a search of publications by the United States Geological Survey and publications and library holdings of the Utah Geological Survey regarding Skull Valley. PFS also consulted with two independent geologists regarding the potential for economic mineralization in the valley. That inquiry reflects that Skull Valley (including the Rail Corridor, ITP and PFSF) contains no known mineral or oil and gas deposits, except for sand and gravel and other commonly occurring deposits. None of these latter types of deposits are located within the Rail Corridor, ITP or PFSF. In addition, this inquiry indicates that Skull Valley has little mineral or oil and gas potential. In particular, the inquiry reveals that Skull Valley has very low potential for the discovery of economic metallic mineral deposits, and there is no reasonable possibility of an open pit metallic mine that would interfere with the proposed rail line operations during the projected life of the PFSF (USGS 1989). As a

result, there will be no impact from construction of the PFSF on known mineral resources.

The terminus of the Rail Corridor and the PFSF are located on the Skull Valley Reservation. Reservation lands are not subject to location of mining claims, and according to the BIA, there are no mineral leases on the Skull Valley Reservation.

There are no mining claims within the Rail Corridor or ITP site, and none has ever been filed on those lands. In addition, only one mining claim has ever been filed on any of the sections of land affected by the Rail Corridor and ITP site -- a 1982 claim located in Section 20, T. 1 N., R. 9 W., approximately one-half mile from the Rail Corridor. The claim was abandoned in 1983.

The only mineral leases ever issued on land affected by the Rail Corridor and ITP site were oil and gas leases, all but one of which have terminated. The one existing lease affects the Rail Corridor within Section 27, T. 3 S., R. 9 W. Under BLM's multiple use concepts, the existence of the oil and gas lease will not preclude construction and operation of the rail line.

The State of Utah owns the minerals underlying one section of land affected by the Rail Corridor, Section 2, T. 5 S., R. 9 W., with the BLM owning the surface of that section. State lands are not subject to location of mining claims. No mineral leases currently affect that section of land, and the only historic leases were oil and gas leases.

4.1.5.1 Imported Materials Required for Construction

The type and quantity of required imported materials necessary for construction of the alternative rail line, ITP, and the PFSF site are provided in Table 4.1-6. PFS does not intend to obtain any required imported construction materials from Federal or Tribal lands, but plans to obtain materials from private, commercial sources in and around the Skull Valley area.